# AUSTRALIAN GEOLOGICAL SURVEY ORGANISATION



AGSO
AUSTRALIAN GEOLOGICAL SURVEY ORGANISATION

Geoscientific Mapping of the Sierras Pampeanas
Argentine-Australia Cooperative Project

Mapeo Geocientifico de las Sierras Pampeanas
Proyecto Argentino-Australiano de cooperación

SECRETARIA DE MINERIA DE LA NACION

**COMMERCIAL - IN - CONFIDENCE**

Argentina

Chile

Océano Atlantico

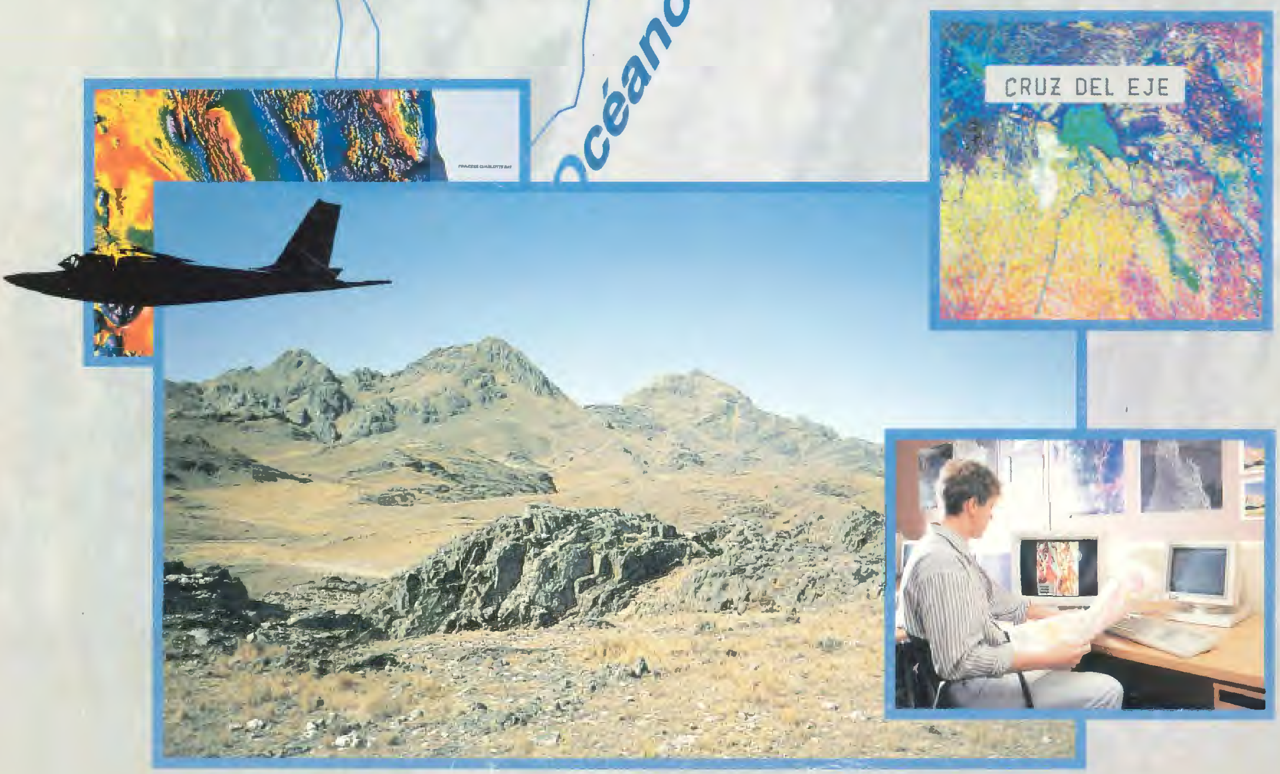

# $^{40}Ar$-$^{39}Ar$ and Rb-Sr GEOCHRONOLOGY FINAL REPORT

*GEOSCIENTIFIC MAPPING OF THE SIERRAS PAMPEANAS ARGENTINE-AUSTRALIA COOPERATIVE PROJECT*

A. Camacho, M.Sc.

AUSTRALIAN GEOLOGICAL SURVEY ORGANISATION

January 1997

## CONTENTS

# 1. INTRODUCTION

This report is the final presentaton of argon-argon and rubidium-strontium geochronological data for samples from the Sierras Septentrionales de Córdoba (Provincia de Córdoba), Sierras de San Luis and Comechingones (Provincias de San Luis and Córdoba), and the Sierras de Chepes and Las Minas (Provincia de La Rioja) areas.

The Geoscientific Mapping of the Sierras Pampeanas is a cooperative project between the Australian Geological Survey Organisation (AGSO) and the Dirección Nacional del Servicio Geológico (DNSG) of the Subsecretaría de Minería, funded by the Government of the Argentine Republic. As a pilot second generation mapping program, the project aims to update the geoscientific knowledge base, provide a modern framework for resource assessment, and promote exploration and development in the region.

The project covers three separate areas totalling 27 000 square kilometres in the southern part of the Sierras Pampeanas, Argentina (Figure 1) where basement Precambrian to Palaeozoic metamorphic and granitic rocks crop out on the eastern margin of the Andean Mobile Belt. The area, well known for its production of industrial and construction materials also contains numerous metallic deposits. Mineral resources include gold and polymetallic (Ag, Pb, and Zn) vein deposits, Ni-Cu sulfide deposits, tungsten, beryllium, lithium, niobium, tantalum, tin, manganese, and chromium. The three areas were selected to provide key information on their geology and mineral potential through the application of integrated geophysical/geological mapping and metallogenic analysis and to provide a continuous section of the major tectonostratigraphic packages comprising the southern Sierras Pampeanas.

As part of the Work Program, geochronological analyses, using U-Pb, Ar-Ar and Rb-Sr techniques of selected samples were undertaken. The aim of the geochronological program is to provide key data to establish the timing of igneous rock crystallisation, major metamorphic/deformation episodes, and mineralising events. The data also allow independent correlation of metamorphic rock packages with numerical age control, assisting geological mapping of the project area, and providing an important database and framework for tectonic interpretation of the Sierras Pampeanas.

In total, 41 samples were collected for geochronological analysis, including samples representative of basement rock types found in the three detailed study areas and samples associated with the mineral occurrence mapping program. All samples submitted for geochronological analysis were petrographically described and analysed for whole-rock major and trace elements.

This report presents $^{40}Ar-^{39}Ar$ data for white mica in eight samples of mineralised and hydrothermally altered rocks; white mica and biotite in five samples of rocks from shear zones; and two white mica samples from pegmatites that intruded synchronous with deformation. Sample location data, petrographic descriptions and whole rock geochemical analyses were reported by Stuart-Smith and others (1996), Sims and others (1996) and Lyons and others (1996), respectively. Brief descriptions of the geological settings of the samples are given in the results for each group of samples, followed by summary comments on $^{40}Ar-^{39}Ar$ ages. Further descriptions of the geology pertaining to the $^{40}Ar-^{39}Ar$ geochronology samples, as well as geological interpretations of the geochronology data in relation to the metallogenic, magmatic and tectonic evolution of the three regions studied, are presented in the Economic Geology sections and other parts of the reports by Sims and others (1997), Lyons and others (1997) and Pieters and others (1997). The results of U-Pb geochronological analyses are presented in Camacho and Ireland (1996, 1997).

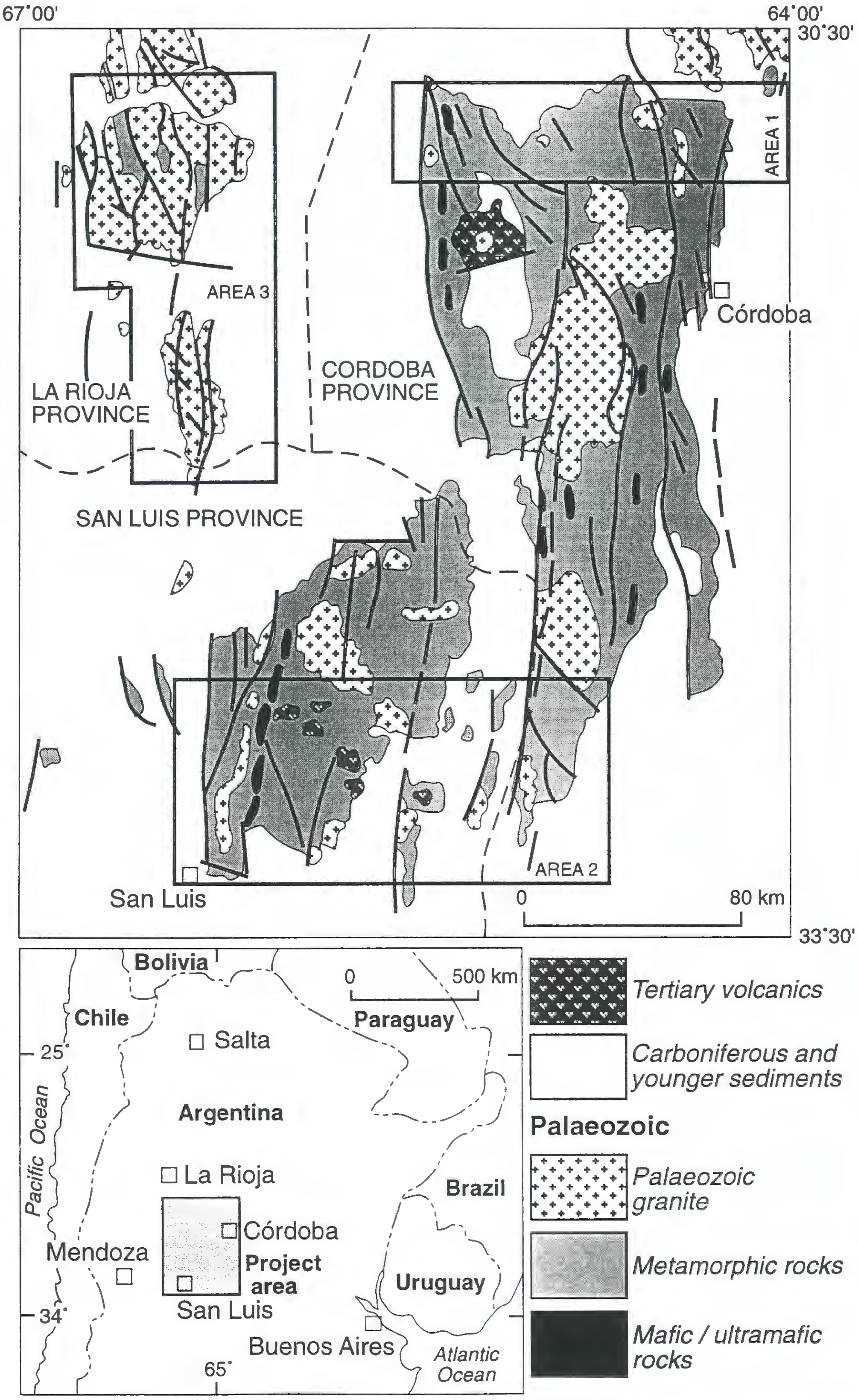


**Figure 1.** *Location of the project area and simplified geological map of the southern Sierras Pampeanas. The three areas of Argentine–Australian cooperative geoscientific mapping are indicated.*

# 2. METHODS

## 2.1 Sample Collection

Representative rock samples were selected during 1995 as part of Field Program 2 (Stuart-Smith and others, 1996). All samples correspond to GPS-located sites recorded using the AGSO field database system, and data are stored in the ARGROC database developed for the project. Samples were split in Argentina with half retained by the Subsecretaría de Minería in Córdoba, and the remainder analysed in Australia.

## 2.2 Sample preparation

Approximately 1 kg of rock was crushed into chips about 2 cm diameter using a jaw crusher. The chips were washed with water to remove any surface contaminants and then crushed to pass 420 mm mesh. Concentrates for all the samples were prepared by AMDEL (Appendix I).

Subsequent procedures to obtain purity > 98% from the concentrates prepared by AMDEL involved vibrating glass and static techniques, Frantz Isodynamic Separator, and separation in heavy liquid of 2.75 -2.96 specific gravity.

## 2.3 Analytical techniques

Irradiation of samples for $^{40}Ar$-$^{39}Ar$ analysis was carried in facility X33 or X34 of the HIFAR reactor of the Australian Nuclear Science and Technology Organisation. All mineral samples were irradiated for 336 hours, with the biotite standard GA 1550 (age of 97.9 Ma; McDougall and Roksandic, 1974) in the central position as described by McDougall and Harrison (1988). Cadmium sleeves, 0.2 mm thick, were placed inside the sample cans to minimise interference from thermal neutrons. Sample cans were rotated 180° three times through the irradiation in order to minimise the effects of the neutron flux gradient in HIFAR.

Biotite, sericite and muscovite were analysed by progressively increasing the temperature from 500 to 1450°C with the gas from each extraction step exposed to Zr-Al getters to remove active gases. Argon was subsequently analysed using a VG Isotech MM1200 gas source mass-spectrometer operating in static mode. Corrections for argon produced by neutron interactions with calcium and potassium were made using the factors determined by Tetley and others (1980). The $^{40}K$ abundance and decay constants recommended by the IUGS Subcommission on Geochronology were used (Steiger and Jäger, 1977). All errors quoted are at the $1\sigma$ level unless stated otherwise.

## 3. RESULTS

Details of the fifteen samples analysed for $^{40}Ar$-$^{39}Ar$ and the corresponding total fusion and step heating age are given in Table 1.

### 3.1 $^{40}Ar$-$^{39}Ar$ on mica associated with mineralisation

#### 3.1.1 SERICITE

Samples A95RS008a, A95RS021c and A95RS028b contain sericite of hydrothermal alteration origin from three mesothermal Au quartz vein deposits in the Sierras de Córdoba. Samples A95RS033 and A95RS047a are from mesothermal Au (Cu, Ag) quartz veins in the Sierra de las Minas, La Rioja. Sericite in all the samples is closely associated with early pyrite-Au mineralisation, and overprints relict metamorphic muscovite derived from the host rocks. Amphibolite facies metamophism in Sierras Septentrionales de Córdoba occurred in the early Cambrian (Lyons and others, 1997; Camacho and Ireland, 1997), whereas in the Sierras de Las Minas and Chepes of La Rioja amphibolite facies metamorphism occurred in the Ordovician (Pieters and others, 1997; Camacho and Ireland, 1997). In all the mesothermal Au deposits the sericite-pyrite-Au assemblages, which formed at about 250-350°C in brittle-ductile shear zone systems, were overprinted by lower temperature hematitic alteration and brittle fracturing (see Skirrow, 1997a, 1997b in Lyons and others, 1997, and Pieters and others, 1997). There is no evidence for white mica growth at this stage.

Data and figures relating to step heating experiments carried out on sericite in mineralised veins are given in Appendix II.

The $^{40}Ar$-$^{39}Ar$ step heating experiments show that the first few steps and the last two steps have Ca/K ratios that are considerably higher than the remainder of the gas. These ages are not considered to have a major geological significance.

The $^{40}Ar$-$^{39}Ar$ step heating of samples A95RS008a, A95RS021c, A95RS028b and A95RS047a gave continuously rising age spectra. Sericite is the fine grained equivalent of muscovite and has a wide range of grain sizes. For this reason, the smaller grains (small domains) may have a lower closure temperature than the larger domains or crystals (e.g. McDougall and Harrison, 1988). Therefore, a monotonically rising age spectrum may reflect the timing in which the different domains closed isotopically during cooling. The maximum apparent age is interpreted to represent the maximum age estimate for the time of initial closure as the formation temperature of the veins and associated hydrothermal alteration is close to the Ar closure temperature of sericite of about 320°C; McDougall and Harrison, 1988). The ages determined from step heating experiments are quoted as an age range (Table 1) because the age spectra for white mica associated with mineralisation are not plateaux.

Sample A95RS033b has an age spectrum that is saddle shaped, reflecting excess argon in the system. The saddle in the spectrum (~390 Ma) is normally interpreted as reflecting the time of crystallisation or final cooling. Sample A95RS068c has a relatively flat spectrum with the ages decreasing slightly with increasing temperature. If the first three steps and last step are excluded, the remainder of the gas yields a mean age of 387 ± 3 Ma.

In summary, samples A95RS008a, A95RS021c and A95RS028b, from Córdoba mesothermal Au deposits, have continuously rising age spectra from about 360 to approximately 380 Ma. The most probable age of sericite crystallisation and, by implication Au mineralisation, corresponds to the older limits of these continuously rising spectra, namely at about 370-380 Ma. The younger parts of the spectra may represent closure of progressively finer grained sericite during cooling of the hydrothermal system, as explained above.

The spectra for samples A95RS033b and A95RS047a, from mesothermal Au (Cu-Ag) quartz veins in La Rioja, are suggestive of sericite crystallisation at about 389-393 Ma. This age is similar to that inferred for sericite associated with Ag-Pb-Zn veins from the El Guaico district of Córdoba (A95RS068c, 386 ± 4 Ma). Taken with the Ar-Ar ages of 363 ± 1 Ma and 366 ± 1 Ma for muscovite associated with W mineralisation in Córdoba and San Luis (see section 3.1.2) the results support the proposal of an early Devonian (~370-393 Ma) Au, Ag, Pb, Zn, W, Cu metallogenic event in the southern Sierras Pampeanas (Skirrow and Sims, 1997; Skirrow 1997a, b, c).

Muscovites extracted from the same samples as sericite have $^{40}Ar$-$^{39}Ar$ total fusion ages that are older than the sericites (Table 1) and are interpreted as being derived from the older surrounding gneisses and schists.

**Table 1.** Sample description and localities of minerals analysed for $^{40}Ar$-$^{39}Ar$ and Rb-Sr.

| Sample no (A95) | Province (Deposit) | Latitude (S) Longitude (W) | Rock type & (Mineral deposit type) | Mineral | Total fusion Age (Ma) | Step heating Age (Ma) | Type of spectra |
|---|---|---|---|---|---|---|---|
| **Micas associated with mineralisation** | | | | | | | |
| RS 008a | Córdoba, San Ignacio | 30.94701<br>64.53076 | Quartz vein<br>(Au) | Sericite | **355 ± 1** | **351 - 370** | Continuosly rising |
| RS 008a | | | | Muscovite | **407 ± 1** | - | |
| RS 021c | Córdoba, Puigari | 31.00314<br>64.81448 | Quartz vein<br>(Au) | Sericite + trace muscovite | **368 ± 1** | **359 - 378** | Continuously rising |
| RS 021c | | | | Muscovite | **408 ± 2** | - | |
| RS 028b | Córdoba, La Bragada | 31.00460<br>64.83318 | Altered gneiss<br>(Au) | Sericite | **370 ± 1** | **364 - 376** | Continuously rising |
| RS 028b | | | | Muscovite | **441 ± 1** | - | |
| RS 033b | La Rioja, Callana VI | 31.69716<br>66.35986 | Altered granite<br>(Au-Cu) | Sericite+ trace muscovite | **393 ± 1** | **~390** | Saddle |
| RS 047a | La Rioja, Vallecito | 31.89430<br>66.29145 | Quartz vein<br>(Au-Cu) | Sericite | **373 ± 2** | **382 - 393** | Continuously rising |
| RS 047a | | | | Muscovite | **426 ± 2** | - | |
| RS 068c | Córdoba, Rara Fortuna | 30.98037<br>65.23002 | Altered gneiss<br>(Ag-Pb-Zn) | Sericite | **385 ± 1** | **386 ± 4** | Flat |
| RS 079b | Córdoba, Agua de Ramón | 30.84688<br>65.37556 | Qtz, tourm vein<br>(W) | Muscovite | **367 ± 1** | **366 ± 1** | Flat |
| RS 101a | San Luis, Loma Blanca | | Qtz, fluor vein<br>(W) | Muscovite | **364 ± 1** | **363 ± 1** | Flat |

### 3.1.2 MUSCOVITE

Sample A95RS079b consists of coarse muscovite from the margin of a quartz-tourmaline vein from Mina Esmeralda in the Aguas de Ramón district of Córdoba. The vein is representative of wolframite-bearing mineralisation hosted mainly by a ?Cambrian to ?Devonian granodiorite stock. Coarse muscovite in sample A95RS101a is from the margin of a scheelite-fluorite-quartz vein cross cutting marble and calcsilicate rocks at the Loma Blanca W deposit, Sierra de Los Morillos, San Luis. These W-bearing veins are interpreted to be broadly synchronous with disseminated scheelite ore in calcsilicate rocks. Muscovite in both samples is proposed to have formed at 400 ± 50°C (Skirrow 1997a, c, in Lyons and others, 1997 and Sims and others, 1997).

Data and figures relating to step heating experiments carried out on muscovites in mineralised veins are given in Appendix III. The $^{40}Ar$-$^{39}Ar$ step heating of samples A95RS079b, and A95RS101a give an overall flat spectra with apparent ages of 366 ± 1 and 363 ± 1 Ma, respectively. These ages are within error of the total fusion ages (Table 1). Given the proposed formation temperatures for muscovites in relation to the Ar closure temperature for muscovite of ~350°C (McDougall and Harrison, 1988), these ages are regarded as dating the ore-vein formation.

**Table 1 (cont).** Sample description and localities of minerals analysed for $^{40}Ar$-$^{39}Ar$ and Rb-Sr.

| Sample no (A95) | Province (Deposit) | Latitude (S) | Longitude (W) | Rock type & (Mineral deposit type) | Mineral | Total fusion Age (Ma) | Step heating Age (Ma) | Type of spectra |
|---|---|---|---|---|---|---|---|---|
| **Micas associated with shear zones** | | | | | | | | |
| JS 086 | San Luis | 33.26173 | 66.17059 | Sheared pegmatite | Fine musc | **375 ± 1** | **374.7 ± 0.5** | Flat |
| JS 086 | San Luis | 33.26173 | 66.17059 | Sheared pegmatite | Coarse musc | **384 ± 1** | - | |
| JS 130 | San Luis | 33.02794 | 65.93205 | Mylonite | Muscovite | **354 ± 1** | **351 - 362** | Continuously rising |
| AC 011b | San Luis | 32.88154 | 66.08597 | Kyanite bearing shear zone | Muscovite | **366 ± 1** | **365.0 ± 0.5** | Flat |
| PP 192b | La Rioja | 31.10252 | 66.33944 | Mylonitised granite | Muscovite | **454 ± 1** | **450 - 462** | Continuously rising |
| PL 230b | Córdoba | 31.04803 | 64.82461 | Mylonite | Biotite | **355 ± 1** | **358.3 ± 0.5** | Flat |
| PL 230b | Córdoba | 31.04803 | 64.82461 | Mylonite | Muscovite | **NA** | **365 - 455** | Continuously rising |
| **Micas associated with pegmatites emplaced synchronous with deformation.** | | | | | | | | |
| *PS 082c | Córdoba | 31.07495 | 64.51052 | Pegmatite | Muscovite | **429 ± 1** | **428.2 ± 0.5** | Flat |
| #AC022b | San Luis | 32.92856 | 65.95210 | Pegmatite | Muscovite | **NA** | - | |

Ages quoted in columns 6 and 7 were determined by $^{40}Ar$-$^{39}Ar$

∗ Sample PS082c was analysed for $^{40}Ar$-$^{39}Ar$ and Rb-Sr isotopes

# Sample AC022b was analysed for Rb-Sr isotopes only

## 3.2 $^{40}Ar$-$^{39}Ar$ on micas associated with shear zones

### 3.2.1 MUSCOVITE

Samples A95AC011b, A95JS086f, A95JS130, A95PL230b and A95PP192b are from shear zones that truncate the early amphibolite facies fabric. In San Luis, there are a series of shear zones that appear to have equilibrated at different crustal levels. Sample A95AC011b is from a kyanite + staurolite + muscovite ± sillimanite bearing shear zone and probably formed at pressures of ~4 kbar or greater. Sample A95JS086f is a greenschist facies shear zone containing metamorphic muscovite and garnet that grew during mylonitisation. Sample A95JS130b, is also from a greenschist facies shear zone system, however with a different shear sense to A95JS086f. Muscovite from these three samples were analysed to determine the ages of these shear zones. Sample A95PP192b is from a mylonitised granite in La Rioja. See next section for Sample A95PL230b.

Data and figures relating to step heating experiments carried out on muscovites that grew during mylonitisation are given in Appendix IV. The $^{40}Ar$-$^{39}Ar$ step heating experiments show that the first few steps and the last two steps have Ca/K ratios that are considerably higher than the remainder of the gas. These ages are not considered to have a major geological significance.

The $^{40}Ar$-$^{39}Ar$ step heating of sample A95AC011b has an age spectrum where the youngest and oldest ages are ~7 Ma apart. Therefore, the age spectrum is this sample is taken to be flat overall, yielding an apparent weighted mean age of 365.0 ± 0.5 Ma.

Sample A95JS086f contains two types of muscovite: a relict pegmatitic coarse grained muscovite and a fine grained muscovite aligned parallel with the mylonitic lineation. The coarse grained muscovite separate yielded a total fusion age that is ~10 Ma older than the fine grained separate (Table 1), and is interpreted as a reset age. $^{40}Ar$-$^{39}Ar$ step heating was only carried out on the fine grained separate (sample A95JS086f). The age spectrum is taken to be overall flat and yields an apparent weighted mean ages of 374.7 ± 0.5 Ma.

The $^{40}Ar$-$^{39}Ar$ step heating of samples A95JS130, and A95PP192b gave continuously rising age spectra. These monotonically rising age spectra may reflect the timing in which the different domains closed isotopically during cooling. The maximum apparent age may be interpreted to represent the maximum age estimate for the time of initial closure. Alternatively, it may reflect partial argon loss during a subsequent event. In summary, sample A95PP192b shows an age range from ~450 to ~462 Ma and sample A95JS130 from ~351 to ~362 Ma.

### 3.2.2 MUSCOVITE and BIOTITE (Sample A95PL230b)

The data and age spectrum relating to the step heating experiments carried out on biotite and muscovite from sample A95PL230b, are given below in Appendix V. The $^{40}Ar$-$^{39}Ar$ step heating experiments show that the first three steps and the last two steps have Ca/K ratios that are considerably higher than the remainder of the gas. These ages are not considered to have a major geological significance.

Biotite is weakly aligned parallel with a mylonitic rodding lineation and is considered to have grown during mylonitisation. The biotite spectrum is overall flat and yields an apparent weighted mean age of 358.3 ± 0.5 Ma.

Muscovite from sample A95PL230b is deformed, and is interpreted as relict grains that grew during amphibolite facies metamorphism in the Cambrian or Ordovician. For this reason, it was separated to determine whether the shear zone attained temperatures > ~320°C (the Ar closure temperature for muscovite). $^{40}Ar$-$^{39}Ar$ step heating gave a continuously rising age spectrum from step 2 at 364.9 ± 0.2 Ma to step 18 at 455.2 ± 2.3 Ma. Therefore, the age spectra is interpreted as a representing partial degassing of relict amphibolite facies muscovite at around 360 Ma, and the temperature during shearing was ~300°C (closure temperature for biotite).

## 3.3 $^{40}Ar$-$^{39}Ar$ and Rb-Sr on micas associated with pegmatites synchronous with deformation

### 3.3.1 MUSCOVITE

Data and figures relating to step heating experiments and Rb-Sr analyses carried out on muscovite associated with pegmatite intrusions coeval with regional metamorphism and deformation are given in Appendix VI.

The $^{40}Ar$-$^{39}Ar$ step heating of samples A95PS082c yields an age spectrum that is overall flat and gives an apparent weighted mean age of 428.2 ± 0.5 Ma.

As the Rb-Sr closure temperature of muscovite is ~500°C, Rb-Sr analyses were carried out on sample A95PS082c as an additional control on the geological interpretation of the $^{40}Ar$-$^{39}Ar$ age and on sample A95AC022b to establish a minimum emplacement age. If the $^{87}Sr/^{86}Sr$ ratio of the analysed muscovites were > 1.5 an age estimate may be obtained independant of the inital $^{87}Sr/^{86}Sr$ ratio. However, the $^{87}Sr/^{86}Sr$ ratio for both muscovites is considerably lower than 1.5. The age variation with changing inital $^{87}Sr/^{86}Sr$ ratio is shown below in Appendix VI. For sample A95PS082c muscovite, an initial $^{87}Sr/^{86}Sr$ of 0.72 would be required in the whole-rock to be comparable to the $^{40}Ar$-$^{39}Ar$ age. Overall, age estimates may not be obtained for either sample unless some estimate of the $^{87}Sr/^{86}Sr$ ratio for pegamtites from both terrains can be made.

## REFERENCES


CAMACHO, A. and IRELAND, T.R., 1996. Geochronology Preliminary Report. Geoscientific Mapping of the Sierras Pampeanas Argentine-Australian Cooperative Project, Australian Geological Survey Organisation, unpublished report.

CAMACHO, A. and IRELAND, T.R., 1997. U-Pb Geochronology: Final report. Geoscientific Mapping of the Sierras Pampeanas Argentine-Australian Cooperative Project, Australian Geological Survey Organisation, unpublished report.

LYONS, P., STUART-SMITH, P.G. and SKIRROW, R.G., 1997. Geology of the Sierras Septentrionales de Córdoba, Provincia de Córdoba - 1:250 000 Geology Map and Report. Geoscientific Mapping of the Sierras Pampeanas Argentine-Australian Cooperative Project, Australian Geological Survey Organisation, unpublished report.

MCDOUGALL, I. and HARRISON, T.M., 1988. Geochronology and Thermochronology by the $^{40}Ar/^{39}Ar$ Method. Oxford University Press, New York.

MCDOUGALL, I. and ROKSANDIC, Z., 1974. Total $^{40}Ar/^{39}Ar$ fusion ages using HIFAR reactor. Journal of the Geological Society of Australia, 21, 81-89.

PIETERS, P., LYONS, P. and SKIRROW, R.G., 1997. Geology of the Sierras de Las Minas and Chepes, Provincia de La Rioja - 1:250 000 Geology Map and Report. Geoscientific Mapping of the Sierras Pampeanas Argentine-Australian Cooperative Project, Australian Geological Survey Organisation, unpublished report.

SIMS, J.P., STUART-SMITH, P.G., LYONS, P. and SKIRROW, R.G., 1997. Geology of the Sierras de San Luis and Comechingones, Provincias de San Luis and Córdoba - 1:250 000 Geology Map and Report. Geoscientific Mapping of the Sierras Pampeanas Argentine-Australian Cooperative Project, Australian Geological Survey Organisation, unpublished report.

SKIRROW, R.G., 1997a. Economic geology, In: LYONS, P., STUART-SMITH, P.G. and SKIRROW, R.G., Geology of the Sierras Septentrionales de Córdoba, Provincia de Córdoba - 1:250 000 Geology Map and Report. Geoscientific Mapping of the Sierras Pampeanas Argentine-Australian Cooperative Project, Australian Geological Survey Organisation, unpublished report.

SKIRROW, R.G., 1997b. Economic geology, In: PIETERS, P., LYONS, P. and SKIRROW, R.G., Geology of the Sierras de Las Minas and Chepes, Provincia de La Rioja - 1:250 000 Geology Map and Report. Geoscientific Mapping of the Sierras Pampeanas Argentine-Australian Cooperative Project, Australian Geological Survey Organisation, unpublished report.

SKIRROW, R.G., 1997c. Economic geology, In: SIMS, J.P., STUART-SMITH, P.G., LYONS, P. and SKIRROW, R.G., Geology of the Sierras de San Luis and Comechingones, Provincias de San Luis and Córdoba - 1:250 000 Geology Map and Report. Geoscientific Mapping of the Sierras Pampeanas Argentine-Australian Cooperative Project, Australian Geological Survey Organisation, unpublished report.

SKIRROW, R.G. and SIMS, J.P, 1997. Metallogenic evolution of the southern Sierras Pampeanas, Argentina. Third National Conference of the Specialist Group in Economic Geology, Canberra, Geological Society of Australia Abstracts, 44: 32-34.

STEIGER, R. and JÄGER, E., 1977. Subcommission on geochronology: Convention on the use of decay constants in geo- and cosmochronology. Earth and Planetary Science Letters, 36, 359-362.

TETLEY, N.I., MCDOUGALL, I. and HEYDEGGER, H.R., 1980. Thermal neutron interferences in the $^{40}Ar/^{39}Ar$ dating technique. Journal of Geophysical Research, 85, 7201-7205.

# APPENDIX I

## AMDEL report on mineral separation

# PREPARATION OF MICA CONCENTRATES FROM SIXTEEN ROCK SAMPLES

## 1. INTRODUCTION

Fourteen rock samples were received from Mr. A. Comacho, AGSO, with a request to prepare mica concentrates of purity exceeding 98%. Each sample was to provide 2 concentrates in the size ranges -60+80 BSS mesh and -80+120 BSS mesh. Thin sections of 12 of the samples were also provided. Subsequently, Mr. Comacho requested that for samples containing both muscovite and sericite, concentrates of both micas should be attempted.

On 9 April, Mr. P. Lyons requested that a muscovite separation be attempted on sample PL 230b, from which a biotite concentrate had already been prepared.

## 2. PROCEDURES

All samples were crushed to pass 36 BSS mesh (420 $\mu$m).

For sample PL 230b, from which biotite was required, the sample was deslimed at 105 $\mu$m and a biotite concentrate prepared from the +105 $\mu$m fraction by froth flotation. This concentrate was cleaned by separation in heavy liquid at 2.96 sp. gr. and finally on a Frantz Isodynamic Separator. The final product was screened at 250, 180 and 125 $\mu$m to produce -250+180 $\mu$m and -180+125 $\mu$m fractions.

The remainder of the samples were to be separated for muscovite and for sericite. These samples were screened at 250, 180 and 125 $\mu$m to produce -250+ 180 $\mu$m and -180+125 $\mu$m fractions. Initial concentration of the mica was made by heavy liquid separations at 2.75 and 2.96 sp. gr. producing mica concentrates in the 2.75-2.96 sp. gr. range.

Subsequent procedures involved using a Frantz Isodynamic Separator and finally heavy liquid separations in a density gradient column in the range 2.75 to 2.96 sp. gr.

## 3. COMMENTS

One sample, RS 070a, was found to be small and almost devoid of micas. The >2.75 sp. gr. products for the -250+180 $\mu$m and -180+125 $\mu$m size range fractions each weighed only 0.18 gram and no further work was attempted.

The samples containing both muscovite and sericite (RS 008a, RS 028b and RS 047a) proved difficult in the separation of the 2 micas and the required >98% purity could not be achieved. In general, the muscovite had a stronger magnetic susceptibility and had a slightly higher specific gravity than the sericite, but overlap of these properties prevented a high purity being achieved. Concentrates of both minerals in the 2 size ranges were prepared for RS 008a and RS 028b, but for RS 047a, concentrates of muscovite and sericite were prepared in the -250+180 μm size range, but only a mixed muscovite/sericite concentrate was prepared from the -180+125 μm fraction.

Sample RS 021c also provided only 0.6 gram of material in the >2.75 sp. gr. product and the final products, with some Fe-staining and quartz/opaque composites, weighed <0.4 grams each.

Sample RS 033b contains strongly Fe-stained sericite and a small percentage of quartz and chert/opaque composites, with the finer grainsize fraction (-180+125 μm) being cleaner than the -250+180 μm product.

Sample RS 068c contains brown, Fe-stained sericite aggregates with some composites with opaques. Rare muscovite is present.

Sample RS 079c concentrates (muscovite) contain traces of tourmaline composites and carbonate. The latter could be removed by acid leaching (HCl) if it is thought that interference at mass 36 from HCl can be avoided.

Sample RS 101a (muscovite) contains a few percent of composite particles with sericite and a few high relief inclusions.

Sample JS 130 is made up of muscovite, often as aggregates and speckled with fine opaque granules.

Sample AC 011b (muscovite) contains some flakes with minute granular opaque inclusions and traces of an intergrown fibrous mineral that may be kyanite or perhaps sillimanite.

Sample PP 192b has muscovite with slight staining and some turbid flakes. There are a few composites with green biotite in the -250+180 μm product.

Sample PL 230b contains only a very low concentration of muscovite, if the thin section provided is representative of the overall sample. Concentrates of muscovite were prepared in three grain size ranges (+250 μm, -250+125 μm and -125+105 μm). The concentrates have a total weight of 0.3 gram and contain a significant proportion of impurities – mainly quartz composites with opaques – and would require further purification by handpicking to reach a purity suitable for geochronology.

The prepared concentrates (32 in total) and the residues will be returned separately.

# APPENDIX II

## $^{40}Ar$-$^{39}Ar$ on sericite associated with mineralisation

$^{40}Ar$-$^{39}Ar$ age spectrum of sample A95RS008a Sericite.

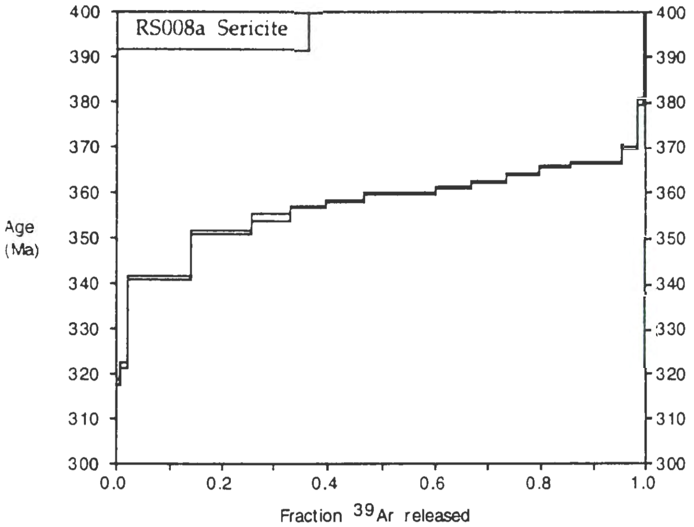


$^{40}Ar$-$^{39}Ar$ step heating data for sample A95RS008a Sericite.

| Temp (°C) | $^{36}Ar$ ($\times10^{-16}$ mol) | $^{37}Ar$ ($\times10^{-16}$ mol) | $^{39}Ar$ ($\times10^{-13}$ mol) | $^{40}Ar$ ($\times10^{-11}$ mol) | $^{40}Ar^*$ (%) | $\frac{^{40}Ar^*}{^{39}K}$ | Cumulative $^{39}Ar$(%) | Age (Ma) ($\pm 1\sigma$) | $\frac{Ca}{K}$ ($\times10^{-3}$) |
|---|---|---|---|---|---|---|---|---|---|
| 500 | 12.530 | 9.575 | 0.527 | 0.178 | 79.1 | 26.662 | 0.54 | 318.1 ± 0.6 | 34.50 |
| 650 | 10.620 | 0.516 | 1.563 | 0.454 | 93.0 | 27.002 | 2.16 | 321.8 ± 0.6 | 0.63 |
| 750 | 8.763 | 0.847 | 11.650 | 3.381 | 99.1 | 28.782 | 14.17 | 341.1 ± 0.4 | 0.14 |
| 810 | 3.397 | 0.850 | 11.200 | 3.342 | 99.6 | 29.715 | 25.72 | 351.2 ± 0.4 | 0.14 |
| 830 | 2.256 | 4.553 | 7.163 | 2.161 | 99.6 | 30.044 | 33.10 | 354.7 ± 0.8 | 1.21 |
| 850 | 2.506 | 0.526 | 6.484 | 1.970 | 99.5 | 30.236 | 39.79 | 356.8 ± 0.2 | 0.15 |
| 870 | 2.262 | 0.977 | 6.512 | 1.986 | 99.6 | 30.372 | 46.50 | 358.2 ± 0.3 | 0.28 |
| 890 | 1.949 | 0.527 | 6.575 | 2.014 | 99.6 | 30.518 | 53.28 | 359.8 ± 0.2 | 0.15 |
| 910 | 3.265 | 0.527 | 6.420 | 1.972 | 99.4 | 30.536 | 59.90 | 360.0 ± 0.2 | 0.16 |
| 930 | 3.289 | 7.532 | 6.466 | 1.993 | 99.4 | 30.640 | 66.57 | 361.1 ± 0.3 | 2.21 |
| 950 | 4.083 | 5.203 | 6.594 | 2.042 | 99.3 | 30.760 | 73.37 | 362.4 ± 0.3 | 1.50 |
| 970 | 3.057 | 2.565 | 6.091 | 1.893 | 99.4 | 30.910 | 79.65 | 364.0 ± 0.2 | 0.80 |
| 990 | 2.175 | 14.550 | 5.731 | 1.788 | 99.6 | 31.055 | 85.56 | 365.5 ± 0.3 | 4.83 |
| 1010 | 2.757 | 5.741 | 5.123 | 1.605 | 99.4 | 31.140 | 90.84 | 366.4 ± 0.2 | 2.13 |
| 1040 | 5.091 | 6.967 | 4.345 | 1.369 | 98.8 | 31.147 | 95.32 | 366.5 ± 0.3 | 3.05 |
| 1080 | 6.717 | 11.800 | 3.132 | 1.007 | 97.9 | 31.477 | 98.55 | 370.0 ± 0.3 | 7.16 |
| 1200 | 7.722 | 17.680 | 1.125 | 0.388 | 94.0 | 32.434 | 99.71 | 380.1 ± 0.5 | 29.90 |
| 1400 | 16.780 | 47.660 | 0.281 | 0.156 | 68.2 | 37.859 | 100.00 | 436.6 ± 2.4 | 322.00 |
| Total | 99.22 | 138.60 | 95.98 | 29.70 | | 30.293 | | 357.4 ± 0.3 | |

$\lambda = 5.543 \times 10^{-10}\ a^{-1}$, $J = 7.2315 \times 10^{-3}$, Flux monitor GA-1550 biotite (97.9 ± 0.7 Ma in age)

$^{40}Ar$-$^{39}Ar$ age spectrum of sample A95RS021c Sericite.

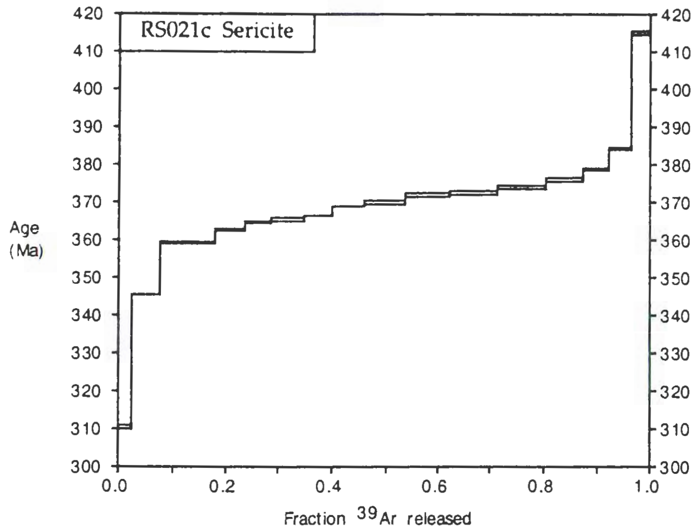


$^{40}Ar$-$^{39}Ar$ step heating data for sample A95RS021c Sericite.

| Temp (°C) | $^{36}Ar$ (x$10^{-16}$ mol) | $^{37}Ar$ (x$10^{-16}$ mol) | $^{39}Ar$ (x$10^{-13}$ mol) | $^{40}Ar$ (x$10^{-11}$ mol) | $^{40}Ar^*$ (%) | $\frac{^{40}Ar^*}{^{39}K}$ | Cumulative $^{39}Ar$(%) | Age (Ma) (± 1σ) | $\frac{Ca}{K}$ (x$10^{-3}$) |
|---|---|---|---|---|---|---|---|---|---|
| 650 | 9.278 | 28.570 | 2.869 | 0.790 | 96.4 | 26.573 | 2.37 | 310.7 ± 0.5 | 18.90 |
| 750 | 3.789 | 192.900 | 6.378 | 1.916 | 99.3 | 29.841 | 7.65 | 345.5 ± 0.2 | 57.50 |
| 810 | 3.127 | 33.430 | 12.380 | 3.867 | 99.7 | 31.146 | 17.90 | 359.2 ± 0.3 | 5.13 |
| 830 | 1.245 | 4.824 | 6.774 | 2.140 | 99.7 | 31.509 | 23.50 | 363.0 ± 0.2 | 1.35 |
| 850 | 0.593 | 1.056 | 5.829 | 1.849 | 99.8 | 31.664 | 28.33 | 364.6 ± 0.2 | 0.34 |
| 870 | 1.125 | 1.071 | 7.837 | 2.494 | 99.8 | 31.750 | 34.81 | 365.5 ± 0.4 | 0.26 |
| 890 | 1.530 | 1.072 | 6.130 | 1.958 | 99.7 | 31.843 | 39.88 | 366.4 ± 0.1 | 0.33 |
| 910 | 0.032 | 11.610 | 7.269 | 2.334 | 99.9 | 32.090 | 45.90 | 369.0 ± 0.1 | 3.03 |
| 930 | 1.892 | 2.152 | 9.277 | 2.995 | 99.7 | 32.194 | 53.58 | 370.1 ± 0.4 | 0.44 |
| 950 | 0.937 | 2.058 | 10.350 | 3.357 | 99.8 | 32.372 | 62.15 | 371.9 ± 0.4 | 0.38 |
| 970 | 2.586 | 2.489 | 11.050 | 3.595 | 99.7 | 32.434 | 71.29 | 372.6 ± 0.4 | 0.43 |
| 990 | 2.764 | 2.193 | 10.840 | 3.540 | 99.7 | 32.569 | 80.26 | 374.0 ± 0.4 | 0.38 |
| 1010 | 2.225 | 1.782 | 8.793 | 2.889 | 99.7 | 32.759 | 87.54 | 376.0 ± 0.4 | 0.38 |
| 1030 | 0.030 | 1.137 | 5.660 | 1.872 | 99.9 | 33.047 | 92.22 | 378.9 ± 0.2 | 0.38 |
| 1080 | 0.361 | 46.050 | 5.294 | 1.778 | 99.9 | 33.547 | 96.60 | 384.1 ± 0.3 | 16.50 |
| 1400 | 0.838 | 64.570 | 4.104 | 1.504 | 99.8 | 36.567 | 100.00 | 415.0 ± 0.3 | 29.90 |
| Total | 32.35 | 396.90 | 120.80 | 38.88 | | 32.072 | | 368.8 ± 0.3 | |

$\lambda = 5.543 \times 10^{-10}\ a^{-1}$, $J = 7.0728 \times 10^{-3}$, Flux monitor GA-1550 biotite (97.9 ± 0.7 Ma in age)

$^{40}Ar$-$^{39}Ar$ age spectrum of sample A95RS028b Sericite

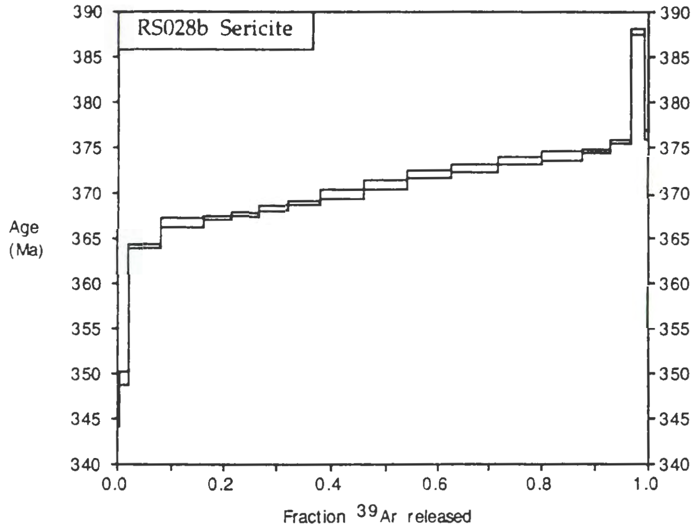


$^{40}Ar$-$^{39}Ar$ step heating data for sample A95RS028b Sericite.

| Temp (°C) | $^{36}Ar$ ($x10^{-16}$ mol) | $^{37}Ar$ ($x10^{-16}$ mol) | $^{39}Ar$ ($x10^{-13}$ mol) | $^{40}Ar$ ($x10^{-11}$ mol) | $^{40}Ar^*$ (%) | $\frac{^{40}Ar^*}{^{39}K}$ | Cumulative $^{39}Ar$(%) | Age (Ma) (± 1σ) | $\frac{Ca}{K}$ ($x10^{-4}$) |
|---|---|---|---|---|---|---|---|---|---|
| 500 | 4.348 | 0.994 | 0.625 | 0.198 | 93.4 | 29.589 | 0.45 | 344.9 ± 0.7 | 30.20 |
| 650 | 4.803 | 0.995 | 2.473 | 0.757 | 98.0 | 30.021 | 2.23 | 349.5 ± 0.7 | 7.64 |
| 750 | 4.045 | 0.995 | 8.197 | 2.589 | 99.5 | 31.416 | 8.12 | 364.2 ± 0.2 | 2.31 |
| 810 | 2.267 | 38.120 | 10.980 | 3.486 | 99.7 | 31.666 | 16.00 | 366.8 ± 0.5 | 66.00 |
| 830 | 1.532 | 1.010 | 7.569 | 2.408 | 99.7 | 31.720 | 21.44 | 367.4 ± 0.2 | 2.53 |
| 850 | 1.384 | 1.011 | 7.177 | 2.285 | 99.7 | 31.756 | 26.60 | 367.7 ± 0.2 | 2.68 |
| 870 | 0.816 | 1.011 | 7.519 | 2.397 | 99.8 | 31.824 | 32.00 | 368.5 ± 0.3 | 2.56 |
| 890 | 1.239 | 1.013 | 8.199 | 2.620 | 99.8 | 31.879 | 37.89 | 369.0 ± 0.2 | 2.35 |
| 910 | 1.601 | 2.110 | 11.240 | 3.601 | 99.8 | 31.963 | 45.97 | 369.9 ± 0.4 | 3.57 |
| 930 | 2.012 | 1.553 | 11.290 | 3.627 | 99.8 | 32.062 | 54.08 | 370.9 ± 0.4 | 2.62 |
| 950 | 1.589 | 2.232 | 11.780 | 3.796 | 99.8 | 32.165 | 62.54 | 372.0 ± 0.4 | 3.60 |
| 970 | 1.262 | 2.249 | 12.350 | 3.986 | 99.8 | 32.225 | 71.41 | 372.6 ± 0.4 | 3.46 |
| 990 | 0.071 | 2.303 | 12.140 | 3.926 | 99.9 | 32.307 | 80.14 | 373.5 ± 0.4 | 3.60 |
| 1010 | 0.060 | 1.968 | 10.560 | 3.419 | 99.9 | 32.364 | 87.72 | 374.1 ± 0.6 | 3.54 |
| 1030 | 0.986 | 1.031 | 7.161 | 2.326 | 99.8 | 32.412 | 92.87 | 374.6 ± 0.3 | 2.74 |
| 1060 | 0.838 | 1.033 | 5.372 | 1.750 | 99.8 | 32.509 | 96.73 | 375.6 ± 0.3 | 3.65 |
| 1200 | 1.007 | 18.330 | 3.734 | 1.261 | 99.7 | 33.675 | 99.41 | 387.7 ± 0.3 | 93.30 |
| 1400 | 2.119 | 133.600 | 0.822 | 0.274 | 97.7 | 32.587 | 100.00 | 376.4 ± 0.5 | 3090.00 |
| Total | 31.98 | 211.50 | 139.20 | 44.71 | | 32.028 | | 370.6 ± 0.4 | |

$\lambda = 5.543 \times 10^{-10}\ a^{-1}$, $J = 7.1198 \times 10^{-3}$, Flux monitor GA-1550 biotite (97.9 ± 0.7 Ma in age)

$^{40}Ar$-$^{39}Ar$ age spectrum of sample A95RS033b Sericite

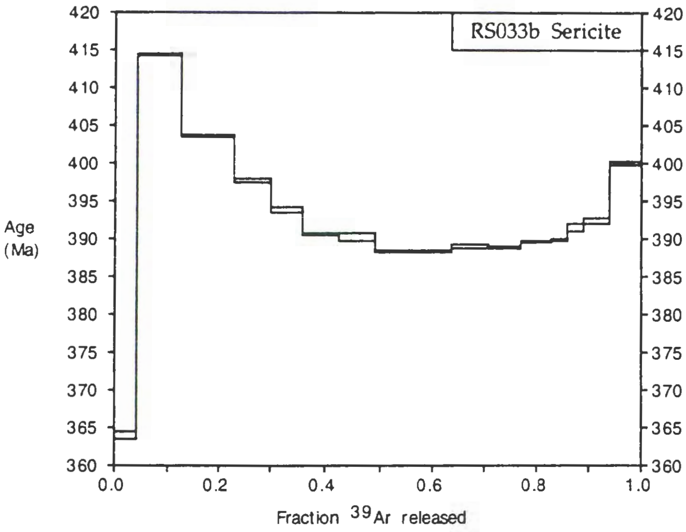


$^{40}Ar$-$^{39}Ar$ step heating data for sample A95RS033b Sericite.

| Temp (°C) | $^{36}Ar$ (x$10^{-16}$ mol) | $^{37}Ar$ (x$10^{-16}$ mol) | $^{39}Ar$ (x$10^{-13}$ mol) | $^{40}Ar$ (x$10^{-11}$ mol) | $^{40}Ar^*$ (%) | $\frac{^{40}Ar^*}{^{39}K}$ | Cumulative $^{39}Ar$(%) | Age (Ma) (± 1s) | $\frac{Ca}{K}$ (x$10^{-3}$) |
|---|---|---|---|---|---|---|---|---|---|
| 650 | 220.300 | 177.600 | 2.695 | 1.621 | 59.8 | 35.993 | 4.10 | 364.0 ± 0.4 | 125.00 |
| 750 | 32.680 | 328.800 | 5.690 | 2.463 | 96.0 | 41.566 | 12.76 | 414.3 ± 0.2 | 110.00 |
| 810 | 13.090 | 5.713 | 6.693 | 2.742 | 98.5 | 40.367 | 22.95 | 403.6 ± 0.2 | 1.62 |
| 830 | 3.608 | 1.143 | 4.421 | 1.768 | 99.3 | 39.723 | 29.68 | 397.8 ± 0.3 | 0.49 |
| 850 | 2.890 | 1.144 | 4.120 | 1.628 | 99.4 | 39.274 | 35.95 | 393.8 ± 0.4 | 0.53 |
| 870 | 4.409 | 4.905 | 4.245 | 1.666 | 99.1 | 38.911 | 42.41 | 390.5 ± 0.1 | 2.20 |
| 890 | 3.125 | 17.220 | 4.407 | 1.723 | 99.4 | 38.870 | 49.12 | 390.2 ± 0.5 | 7.42 |
| 910 | 4.580 | 12.100 | 4.694 | 1.830 | 99.2 | 38.680 | 56.27 | 388.4 ± 0.1 | 4.90 |
| 930 | 4.609 | 11.360 | 4.704 | 1.834 | 99.2 | 38.663 | 63.43 | 388.3 ± 0.1 | 4.59 |
| 950 | 3.975 | 1.163 | 4.575 | 1.785 | 99.3 | 38.738 | 70.39 | 389.0 ± 0.3 | 0.48 |
| 970 | 4.091 | 1.163 | 4.188 | 1.635 | 99.2 | 38.733 | 76.77 | 388.9 ± 0.2 | 0.53 |
| 990 | 4.841 | 1.164 | 3.872 | 1.518 | 99.0 | 38.814 | 82.66 | 389.7 ± 0.2 | 0.57 |
| 990 | 3.319 | 12.150 | 2.216 | 0.871 | 98.8 | 38.830 | 86.04 | 389.8 ± 0.2 | 10.40 |
| 1010 | 2.737 | 8.765 | 2.141 | 0.844 | 99.0 | 39.011 | 89.30 | 391.4 ± 0.6 | 7.78 |
| 1050 | 6.666 | 10.560 | 3.225 | 1.282 | 98.4 | 39.115 | 94.21 | 392.4 ± 0.4 | 6.22 |
| 1400 | 34.750 | 1380.000 | 3.808 | 1.623 | 93.7 | 39.954 | 100.00 | 399.9 ± 0.3 | 689.00 |
| Total | 349.70 | 1975.00 | 65.69 | 26.83 | | 39.252 | | 393.6 ± 0.3 | |

$\lambda = 5.543 \times 10^{-10}\ a^{-1}$, $J = 6.2113 \times 10^{-3}$, Flux monitor GA-1550 biotite (97.9 ± 0.7 Ma in age)

$^{40}Ar$-$^{39}Ar$ age spectrum of sample A95RS047a Sericite.

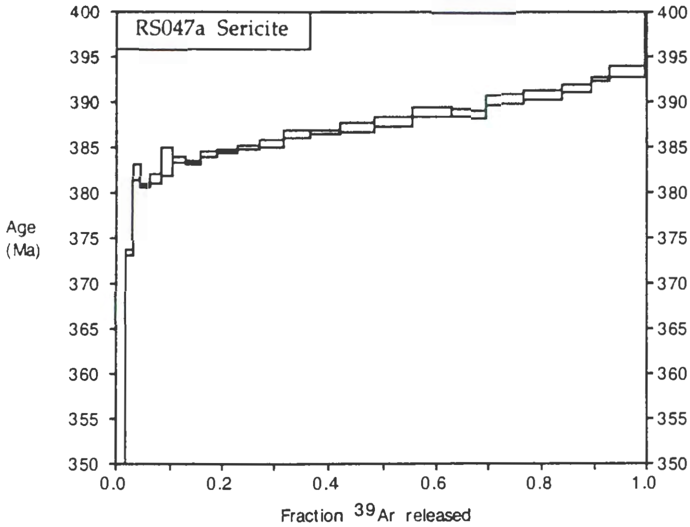


$^{40}Ar$-$^{39}Ar$ step heating data for sample A95RS047a Sericite.

| Temp (°C) | $^{36}Ar$ ($\times10^{-16}$ mol) | $^{37}Ar$ ($\times10^{-16}$ mol) | $^{39}Ar$ ($\times10^{-13}$ mol) | $^{40}Ar$ ($\times10^{-11}$ mol) | $^{40}Ar^*$ (%) | $\frac{^{40}Ar^*}{^{39}K}$ | Cumulative $^{39}Ar$(%) | Age (Ma) ($\pm 1\sigma$) | $\frac{Ca}{K}$ ($\times10^{-4}$) |
|---|---|---|---|---|---|---|---|---|---|
| 500 | 20.580 | 6.813 | 0.718 | 0.260 | 76.6 | 27.761 | 0.47 | 322.8 ± 0.9 | 180.00 |
| 550 | 9.539 | 17.540 | 0.745 | 0.236 | 88.0 | 27.899 | 0.95 | 324.3 ± 2.1 | 448.00 |
| 600 | 7.259 | 5.317 | 1.257 | 0.402 | 94.6 | 30.259 | 1.77 | 349.2 ± 0.7 | 80.30 |
| 650 | 6.098 | 9.302 | 2.368 | 0.790 | 97.6 | 32.589 | 3.31 | 373.5 ± 0.3 | 74.60 |
| 670 | 1.523 | 0.469 | 2.159 | 0.727 | 99.3 | 33.440 | 4.72 | 382.3 ± 0.8 | 4.13 |
| 690 | 2.988 | 5.906 | 2.560 | 0.862 | 98.9 | 33.298 | 6.39 | 380.9 ± 0.2 | 43.80 |
| 710 | 3.626 | 8.932 | 3.080 | 1.039 | 98.9 | 33.362 | 8.39 | 381.5 ± 0.5 | 55.10 |
| 730 | 1.080 | 9.700 | 3.084 | 1.039 | 99.6 | 33.555 | 10.40 | 383.5 ± 1.6 | 59.80 |
| 750 | 1.829 | 0.496 | 4.007 | 1.351 | 99.5 | 33.561 | 13.01 | 383.6 ± 0.3 | 2.35 |
| 770 | 2.321 | 2.198 | 4.443 | 1.498 | 99.5 | 33.535 | 15.91 | 383.3 ± 0.2 | 9.40 |
| 790 | 1.567 | 18.050 | 4.916 | 1.659 | 99.6 | 33.625 | 19.11 | 384.2 ± 0.3 | 69.70 |
| 810 | 1.333 | 0.497 | 5.528 | 1.866 | 99.7 | 33.657 | 22.71 | 384.6 ± 0.2 | 1.71 |
| 830 | 1.426 | 3.982 | 6.427 | 2.172 | 99.7 | 33.703 | 26.90 | 385.0 ± 0.2 | 11.80 |
| 850 | 1.954 | 3.914 | 7.135 | 2.415 | 99.7 | 33.737 | 31.55 | 385.4 ± 0.4 | 10.40 |
| 870 | 0.984 | 0.498 | 7.824 | 2.652 | 99.8 | 33.836 | 36.64 | 386.4 ± 0.4 | 1.21 |
| 890 | 1.417 | 0.499 | 8.368 | 2.841 | 99.8 | 33.871 | 42.09 | 386.8 ± 0.2 | 1.13 |
| 910 | 1.644 | 0.770 | 9.534 | 3.241 | 99.8 | 33.913 | 48.30 | 387.2 ± 0.5 | 1.53 |
| 930 | 2.401 | 2.884 | 10.930 | 3.724 | 99.7 | 33.975 | 55.42 | 387.8 ± 0.5 | 5.01 |
| 950 | 1.316 | 0.933 | 11.270 | 3.849 | 99.8 | 34.077 | 62.77 | 388.9 ± 0.5 | 1.57 |
| 970 | 4.349 | 0.889 | 10.460 | 3.577 | 99.6 | 34.063 | 69.58 | 388.7 ± 0.4 | 1.62 |
| 990 | 1.870 | 0.896 | 10.800 | 3.704 | 99.8 | 34.214 | 76.61 | 390.3 ± 0.5 | 1.58 |
| 1010 | 4.043 | 0.865 | 11.050 | 3.801 | 99.6 | 34.256 | 83.81 | 390.7 ± 0.5 | 1.49 |
| 1030 | 2.928 | 5.965 | 8.586 | 2.958 | 99.6 | 34.327 | 89.41 | 391.4 ± 0.4 | 13.20 |
| 1050 | 2.272 | 4.851 | 5.711 | 1.975 | 99.6 | 34.432 | 93.13 | 392.5 ± 0.2 | 16.10 |
| 1150 | 7.842 | 114.700 | 10.210 | 3.549 | 99.3 | 34.507 | 99.78 | 393.3 ± 0.6 | 213.00 |
| 1400 | 6.820 | 715.300 | 0.344 | 0.179 | 89.1 | 46.377 | 100.00 | 510.9 ± 1.8 | 39600.00 |
| Total | 101.00 | 942.10 | 153.50 | 52.37 | | 33.890 | | 387.0 ± 0.5 | |

$\lambda = 5.543 \times 10^{-10}\ a^{-1}$, $J = 7.0589 \times 10^{-3}$, Flux monitor GA-1550 biotite (97.9 ± 0.7 Ma in age)

$^{40}Ar$-$^{39}Ar$ age spectrum of sample A95RS068c Sericite.

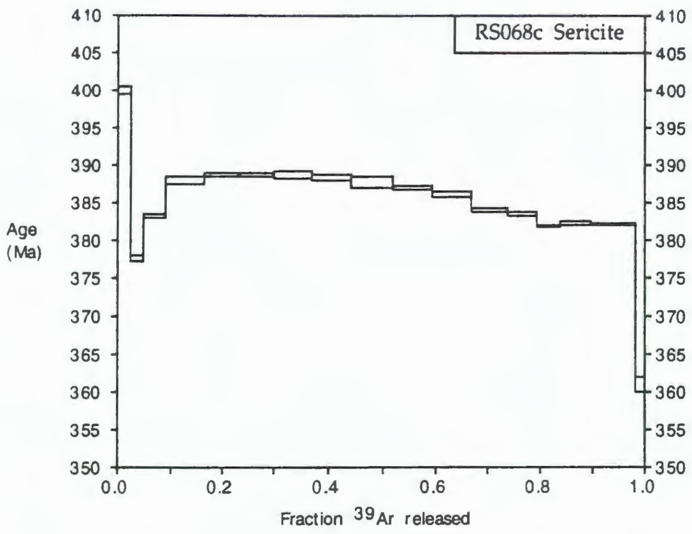


$^{40}Ar$-$^{39}Ar$ step heating data for sample A95RS068c Sericite.

| Temp (°C) | $^{36}Ar$ ($\times10^{-16}$ mol) | $^{37}Ar$ ($\times10^{-16}$ mol) | $^{39}Ar$ ($\times10^{-13}$ mol) | $^{40}Ar$ ($\times10^{-11}$ mol) | $^{40}Ar^*$ (%) | $\frac{^{40}Ar^*}{^{39}K}$ | Cumulative $^{39}Ar$(%) | Age (Ma) ($\pm 1\sigma$) | $\frac{Ca}{K}$ ($\times10^{-3}$) |
|---|---|---|---|---|---|---|---|---|---|
| 500 | 20.060 | 0.432 | 1.899 | 0.790 | 92.4 | 38.453 | 2.56 | 400.1 ± 0.5 | 0.43 |
| 550 | 8.542 | 22.060 | 1.623 | 0.611 | 95.8 | 36.073 | 4.76 | 377.7 ± 0.4 | 25.80 |
| 600 | 8.175 | 7.982 | 3.169 | 1.187 | 97.9 | 36.660 | 9.04 | 383.3 ± 0.3 | 4.79 |
| 650 | 6.017 | 6.007 | 5.605 | 2.102 | 99.1 | 37.161 | 16.61 | 388.0 ± 0.4 | 2.04 |
| 670 | 3.907 | 8.366 | 4.790 | 1.797 | 99.3 | 37.253 | 23.07 | 388.8 ± 0.2 | 3.32 |
| 690 | 3.971 | 4.651 | 4.885 | 1.833 | 99.3 | 37.246 | 29.67 | 388.8 ± 0.2 | 1.81 |
| 710 | 2.608 | 0.435 | 5.207 | 1.948 | 99.5 | 37.245 | 36.70 | 388.8 ± 0.6 | 0.16 |
| 730 | 2.465 | 3.965 | 5.520 | 2.062 | 99.6 | 37.206 | 44.16 | 388.4 ± 0.5 | 1.36 |
| 750 | 1.300 | 5.732 | 5.627 | 2.095 | 99.7 | 37.133 | 51.76 | 387.7 ± 0.8 | 1.94 |
| 770 | 1.036 | 0.442 | 5.637 | 2.094 | 99.8 | 37.066 | 59.37 | 387.1 ± 0.3 | 0.15 |
| 790 | 1.069 | 3.414 | 5.529 | 2.048 | 99.8 | 36.965 | 66.83 | 386.1 ± 0.4 | 1.17 |
| 810 | 1.681 | 0.443 | 4.980 | 1.836 | 99.7 | 36.747 | 73.56 | 384.1 ± 0.3 | 0.17 |
| 830 | 1.750 | 0.443 | 4.164 | 1.533 | 99.6 | 36.678 | 79.18 | 383.4 ± 0.3 | 0.20 |
| 850 | 3.035 | 6.461 | 3.451 | 1.270 | 99.2 | 36.507 | 83.84 | 381.8 ± 0.2 | 3.56 |
| 900 | 3.260 | 13.140 | 4.492 | 1.653 | 99.3 | 36.555 | 89.91 | 382.3 ± 0.3 | 5.56 |
| 1000 | 13.210 | 15.980 | 6.049 | 2.251 | 98.2 | 36.546 | 98.08 | 382.2 ± 0.2 | 5.02 |
| 1400 | 58.180 | 127.000 | 1.425 | 0.661 | 74.0 | 34.313 | 100.00 | 361.0 ± 0.9 | 169.00 |
| Total | 140.30 | 227.00 | 74.05 | 27.77 | | 36.918 | | 385.7 ± 0.4 | |

$\lambda = 5.543 \times 10^{-10}\ a^{-1}$, $J = 6.4563 \times 10^{-3}$, Flux monitor GA-1550 biotite (97.9 ± 0.7 Ma in age)

# APPENDIX III

## $^{40}Ar$-$^{39}Ar$ on muscovite associated with mineralisation

$^{40}Ar$-$^{39}Ar$ age spectrum of sample A95RS079b Muscovite.

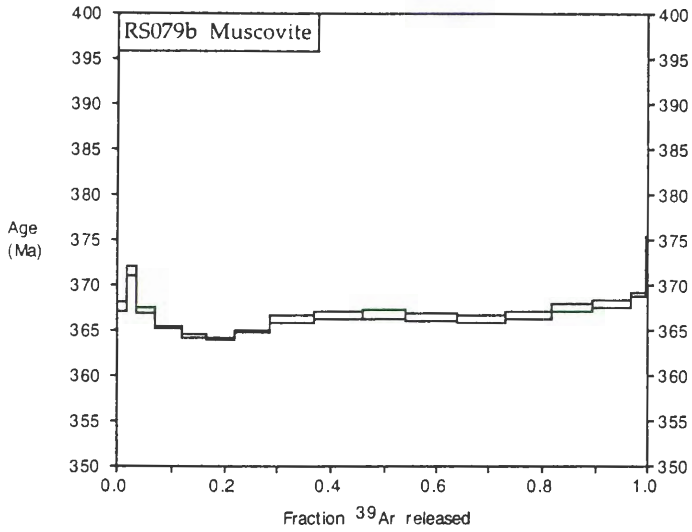


$^{40}Ar$-$^{39}Ar$ step heating data for sample A95RS079b Muscovite.

| Temp (°C) | $^{36}Ar$ ($\times10^{-15}$ mol) | $^{37}Ar$ ($\times10^{-16}$ mol) | $^{39}Ar$ ($\times10^{-13}$ mol) | $^{40}Ar$ ($\times10^{-11}$ mol) | $^{40}Ar^*$ (%) | $\frac{^{40}Ar^*}{^{39}K}$ | Cumulative $^{39}Ar$(%) | Age (Ma) ($\pm 1\sigma$) | $\frac{Ca}{K}$ ($\times10^{-3}$) |
|---|---|---|---|---|---|---|---|---|---|
| 700 | 2.621 | 161.100 | 1.796 | 0.666 | 88.3 | 32.723 | 1.75 | 367.7 ± 0.5 | 170.00 |
| 750 | 0.598 | 30.440 | 1.976 | 0.673 | 97.3 | 33.110 | 3.68 | 371.6 ± 0.5 | 29.30 |
| 800 | 0.974 | 20.760 | 3.424 | 1.149 | 97.4 | 32.681 | 7.02 | 367.2 ± 0.3 | 11.50 |
| 840 | 1.580 | 28.810 | 4.893 | 1.637 | 97.1 | 32.488 | 11.80 | 365.3 ± 0.1 | 11.20 |
| 860 | 1.591 | 11.800 | 4.862 | 1.624 | 97.0 | 32.404 | 16.54 | 364.4 ± 0.2 | 4.61 |
| 880 | 1.912 | 3.279 | 5.485 | 1.833 | 96.8 | 32.372 | 21.89 | 364.1 ± 0.2 | 1.14 |
| 900 | 2.142 | 0.656 | 6.533 | 2.185 | 97.0 | 32.452 | 28.27 | 364.9 ± 0.2 | 0.19 |
| 920 | 2.063 | 2.149 | 8.673 | 2.890 | 97.8 | 32.593 | 36.73 | 366.3 ± 0.4 | 0.47 |
| 940 | 1.658 | 1.218 | 9.434 | 3.130 | 98.4 | 32.628 | 45.93 | 366.7 ± 0.4 | 0.25 |
| 960 | 1.695 | 8.095 | 8.369 | 2.784 | 98.1 | 32.637 | 54.10 | 366.8 ± 0.5 | 1.84 |
| 990 | 2.492 | 6.682 | 9.931 | 3.315 | 97.7 | 32.615 | 63.79 | 366.6 ± 0.4 | 1.28 |
| 1020 | 2.540 | 1.012 | 9.347 | 3.124 | 97.5 | 32.589 | 72.91 | 366.3 ± 0.4 | 0.21 |
| 1050 | 2.640 | 1.069 | 9.003 | 3.018 | 97.3 | 32.626 | 81.70 | 366.7 ± 0.4 | 0.23 |
| 1080 | 1.976 | 0.980 | 8.013 | 2.682 | 97.7 | 32.711 | 89.51 | 367.5 ± 0.4 | 0.23 |
| 1110 | 1.091 | 21.790 | 7.472 | 2.481 | 98.6 | 32.752 | 96.80 | 368.0 ± 0.4 | 5.54 |
| 1140 | 0.255 | 20.540 | 3.093 | 1.024 | 99.2 | 32.848 | 99.82 | 368.9 ± 0.2 | 12.60 |
| 1400 | 0.061 | 0.670 | 0.181 | 0.062 | 97.0 | 33.235 | 100.00 | 372.9 ± 2.7 | 7.03 |
| Total | 27.89 | 321.00 | 102.50 | 34.28 |  | 32.614 |  | 366.6 ± 0.4 |  |

$\lambda = 5.543 \times 10^{-10}\ a^{-1}$, $J = 6.9076 \times 10^{-3}$, Flux monitor GA-1550 biotite (97.9 ± 0.7 Ma in age)

$^{40}Ar$-$^{39}Ar$ age spectrum of sample A95RS101a Muscovite.

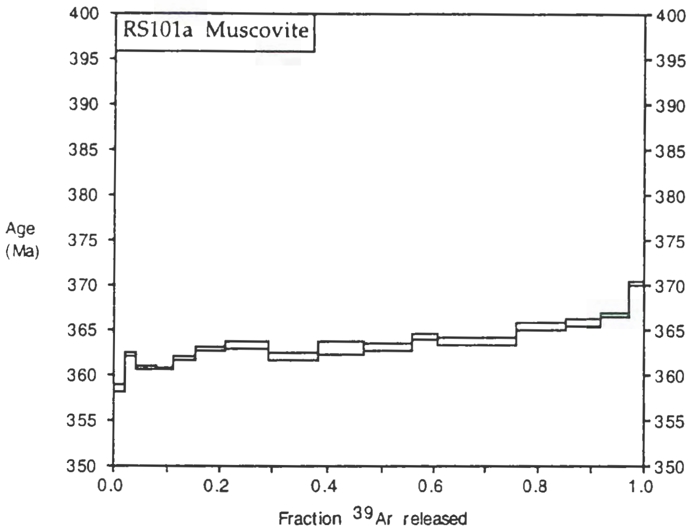


$^{40}Ar$-$^{39}Ar$ step heating data for sample A95RS101a Muscovite.

| Temp (°C) | $^{36}Ar$ (x$10^{-15}$ mol) | $^{37}Ar$ (x$10^{-16}$ mol) | $^{39}Ar$ (x$10^{-13}$ mol) | $^{40}Ar$ (x$10^{-11}$ mol) | $^{40}Ar^*$ (%) | $\frac{^{40}Ar^*}{^{39}K}$ | Cumulative $^{39}Ar$(%) | Age (Ma) (± 1σ) | $\frac{Ca}{K}$ (x$10^{-3}$) |
|---|---|---|---|---|---|---|---|---|---|
| 750 | 27.200 | 31.070 | 2.323 | 0.845 | 90.4 | 32.892 | 2.08 | 358.5± 0.4 | 25.40 |
| 800 | 6.785 | 31.680 | 2.507 | 0.855 | 97.6 | 33.287 | 4.33 | 362.4 ± 0.2 | 24.00 |
| 850 | 10.340 | 0.915 | 4.015 | 1.362 | 97.7 | 33.142 | 7.93 | 360.9 ± 0.2 | 0.43 |
| 870 | 10.910 | 26.440 | 3.836 | 1.304 | 97.4 | 33.121 | 11.37 | 360.7 ± 0.2 | 13.10 |
| 890 | 13.590 | 33.270 | 4.488 | 1.533 | 97.3 | 33.233 | 15.40 | 361.8 ± 0.2 | 14.10 |
| 910 | 15.880 | 9.786 | 6.327 | 2.158 | 97.7 | 33.341 | 21.07 | 362.9 ± 0.2 | 2.94 |
| 930 | 16.330 | 28.790 | 9.073 | 3.080 | 98.4 | 33.382 | 29.21 | 363.3 ± 0.4 | 6.03 |
| 950 | 12.810 | 20.750 | 9.971 | 3.357 | 98.8 | 33.263 | 38.15 | 362.1 ± 0.4 | 3.95 |
| 970 | 10.750 | 13.830 | 9.567 | 3.226 | 98.9 | 33.356 | 46.73 | 363.0 ± 0.7 | 2.75 |
| 990 | 14.220 | 1.474 | 10.230 | 3.458 | 98.7 | 33.372 | 55.91 | 363.2 ± 0.4 | 0.27 |
| 1020 | 6.692 | 0.935 | 5.195 | 1.760 | 98.8 | 33.478 | 60.56 | 364.2 ± 0.3 | 0.34 |
| 1050 | 28.500 | 92.870 | 17.140 | 5.818 | 98.5 | 33.434 | 75.93 | 363.8 ± 0.4 | 10.30 |
| 1080 | 10.480 | 1.878 | 10.370 | 3.516 | 99.0 | 33.591 | 85.23 | 365.4 ± 0.4 | 0.34 |
| 1100 | 5.771 | 55.950 | 7.650 | 2.592 | 99.3 | 33.636 | 92.09 | 365.8 ± 0.4 | 13.90 |
| 1120 | 2.265 | 0.989 | 5.673 | 1.921 | 99.6 | 33.721 | 97.18 | 366.6 ± 0.3 | 0.33 |
| 1400 | 1.205 | 55.430 | 3.145 | 1.077 | 99.6 | 34.090 | 100.00 | 370.3 ± 0.2 | 33.50 |
| Total | 193.70 | 406.10 | 111.50 | 37.86 | | 33.417 | | 363.6 ± 0.4 | |

$\lambda = 5.543 \times 10^{-10}\ a^{-1}$, $J = 6.6826 \times 10^{-3}$, Flux monitor GA-1550 biotite (97.9 ± 0.7 Ma in age)

# APPENDIX IV

## $^{40}Ar$-$^{39}Ar$ on muscovite associated with shear zones

$^{40}Ar$-$^{39}Ar$ age spectrum of sample A95JS086f Muscovite.

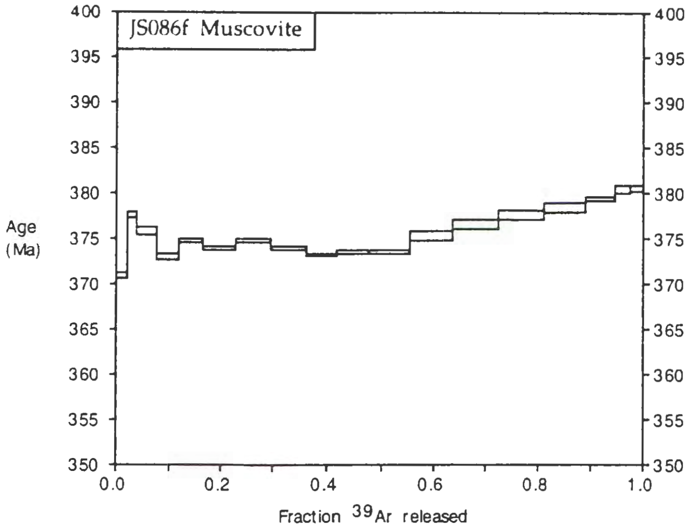


$^{40}Ar$-$^{39}Ar$ step heating data for sample A95JS086f Muscovite.

| Temp (°C) | $^{36}Ar$ ($\times10^{-16}$ mol) | $^{37}Ar$ ($\times10^{-16}$ mol) | $^{39}Ar$ ($\times10^{-13}$ mol) | $^{40}Ar$ ($\times10^{-11}$ mol) | $^{40}Ar^*$ (%) | $\frac{^{40}Ar^*}{^{39}K}$ | Cumulative $^{39}Ar$(%) | Age (Ma) ($\pm 1\sigma$) | $\frac{Ca}{K}$ ($\times10^{-3}$) |
|---|---|---|---|---|---|---|---|---|---|
| 750 | 16.840 | 7.307 | 2.236 | 0.797 | 93.7 | 33.405 | 1.99 | 370.9 ± 0.3 | 6.21 |
| 800 | 4.232 | 20.340 | 2.167 | 0.752 | 98.3 | 34.077 | 3.92 | 377.6 ± 0.3 | 17.80 |
| 850 | 5.220 | 24.930 | 4.271 | 1.464 | 98.9 | 33.893 | 7.73 | 375.8 ± 0.4 | 11.10 |
| 870 | 6.829 | 20.200 | 4.570 | 1.557 | 98.6 | 33.616 | 11.80 | 373.0 ± 0.3 | 8.40 |
| 890 | 5.192 | 1.189 | 5.454 | 1.860 | 99.1 | 33.795 | 16.66 | 374.8 ± 0.3 | 0.41 |
| 910 | 7.543 | 1.192 | 6.861 | 2.337 | 99.0 | 33.714 | 22.78 | 374.0 ± 0.1 | 0.33 |
| 930 | 5.136 | 0.170 | 7.478 | 2.544 | 99.3 | 33.788 | 29.44 | 374.7 ± 0.2 | 0.04 |
| 950 | 4.526 | 1.193 | 7.364 | 2.498 | 99.4 | 33.709 | 36.00 | 373.9 ± 0.2 | 0.31 |
| 970 | 4.573 | 1.194 | 6.442 | 2.182 | 99.3 | 33.639 | 41.74 | 373.2 ± 0.2 | 0.35 |
| 990 | 4.464 | 1.195 | 6.812 | 2.308 | 99.3 | 33.668 | 47.81 | 373.5 ± 0.2 | 0.33 |
| 1020 | 5.944 | 20.430 | 8.721 | 2.956 | 99.3 | 33.670 | 55.58 | 373.5 ± 0.1 | 4.45 |
| 1040 | 4.191 | 2.179 | 9.060 | 3.082 | 99.5 | 33.850 | 63.66 | 375.3 ± 0.6 | 0.46 |
| 1060 | 4.979 | 66.200 | 9.668 | 3.301 | 99.5 | 33.966 | 72.27 | 376.5 ± 0.5 | 13.00 |
| 1080 | 3.535 | 2.294 | 9.799 | 3.352 | 99.6 | 34.077 | 81.01 | 377.6 ± 0.5 | 0.45 |
| 1100 | 2.955 | 33.560 | 9.161 | 3.141 | 99.6 | 34.163 | 89.17 | 378.5 ± 0.5 | 6.96 |
| 1120 | 1.597 | 44.300 | 6.288 | 2.161 | 99.7 | 34.262 | 94.77 | 379.5 ± 0.2 | 13.40 |
| 1140 | 0.242 | 75.050 | 3.154 | 1.085 | 99.9 | 34.361 | 97.58 | 380.5 ± 0.4 | 45.20 |
| 1400 | 1.503 | 468.400 | 2.712 | 0.937 | 99.5 | 34.361 | 100.00 | 380.5 ± 0.3 | 328.00 |
| Total | 89.50 | 791.40 | 112.20 | 38.31 | | 33.881 | | 375.7 ± 0.3 | |

$\lambda = 5.543 \times 10^{-10}\ a^{-1}$, $J = 6.8325 \times 10^{-3}$, Flux monitor GA-1550 biotite (97.9 ± 0.7 Ma in age)

$^{40}Ar$-$^{39}Ar$ age spectrum of sample A95AC011b Muscovite.

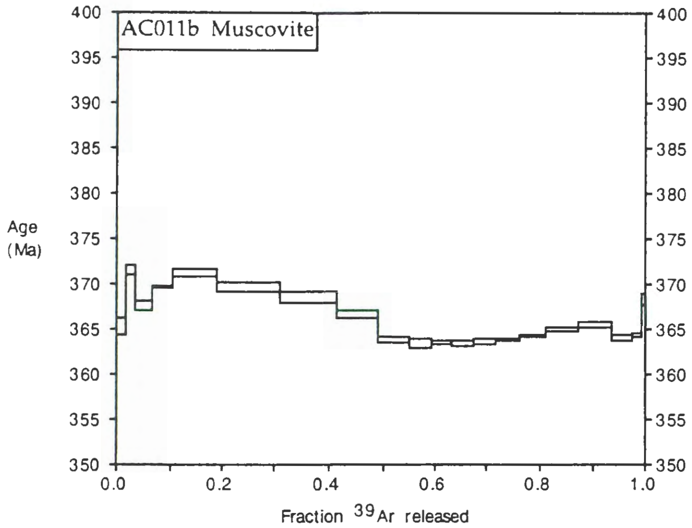


$^{40}Ar$-$^{39}Ar$ step heating data for sample A95AC011b Muscovite.

| Temp (°C) | $^{36}Ar$ (x$10^{-15}$ mol) | $^{37}Ar$ (x$10^{-16}$ mol) | $^{39}Ar$ (x$10^{-13}$ mol) | $^{40}Ar$ (x$10^{-11}$ mol) | $^{40}Ar^*$ (%) | $\frac{^{40}Ar^*}{^{39}K}$ | Cumulative $^{39}Ar$(%) | Age (Ma) (± 1σ) | $\frac{Ca}{K}$ (x$10^{-3}$) |
|---|---|---|---|---|---|---|---|---|---|
| 700 | 2.777 | 6.867 | 1.580 | 0.602 | 86.3 | 32.893 | 1.65 | 365.4 ± 1.0 | 8.26 |
| 750 | 1.446 | 0.607 | 1.733 | 0.624 | 93.1 | 33.514 | 3.46 | 371.6 ± 0.5 | 0.67 |
| 800 | 2.570 | 4.92 | 3.013 | 1.074 | 92.9 | 33.115 | 6.60 | 367.6 ± 0.5 | 3.10 |
| 820 | 2.848 | 0.615 | 3.769 | 1.341 | 93.6 | 33.321 | 10.53 | 369.7 ± 0.2 | 0.31 |
| 840 | 3.322 | 0.939 | 8.067 | 2.800 | 96.4 | 33.471 | 18.95 | 371.2 ± 0.4 | 0.22 |
| 860 | 2.360 | 1.287 | 11.39 | 3.869 | 98.1 | 33.318 | 30.83 | 369.7 ± 0.5 | 0.22 |
| 880 | 1.459 | 1.052 | 10.09 | 3.395 | 98.7 | 33.205 | 41.36 | 368.5 ± 0.6 | 0.20 |
| 900 | 1.020 | 0.891 | 7.573 | 2.533 | 98.7 | 33.020 | 49.26 | 366.7 ± 0.5 | 0.22 |
| 920 | 1.180 | 0.353 | 5.694 | 1.901 | 98.1 | 32.740 | 55.20 | 363.9 ± 0.3 | 0.12 |
| 950 | 1.168 | 2.828 | 3.865 | 1.300 | 97.3 | 32.703 | 59.23 | 363.5 ± 0.5 | 1.39 |
| 980 | 1.416 | 11.14 | 3.758 | 1.272 | 96.6 | 32.709 | 63.15 | 363.5 ± 0.2 | 5.63 |
| 1010 | 1.614 | 0.620 | 3.905 | 1.326 | 96.3 | 32.693 | 67.22 | 363.4 ± 0.3 | 0.30 |
| 1040 | 1.664 | 14.65 | 4.317 | 1.463 | 96.6 | 32.717 | 71.73 | 363.6 ± 0.3 | 6.45 |
| 1060 | 1.473 | 9.62 | 4.128 | 1.396 | 96.8 | 32.734 | 76.03 | 363.8 ± 0.1 | 4.43 |
| 1080 | 1.619 | 0.630 | 4.732 | 1.601 | 96.9 | 32.784 | 80.97 | 364.3 ± 0.2 | 0.25 |
| 1120 | 1.663 | 10.35 | 5.970 | 2.013 | 97.5 | 32.862 | 87.20 | 365.1 ± 0.2 | 3.29 |
| 1120 | 1.151 | 5.223 | 6.139 | 2.056 | 98.3 | 32.910 | 93.60 | 365.6 ± 0.3 | 1.62 |
| 1140 | 0.489 | 3.784 | 3.868 | 1.283 | 98.8 | 32.762 | 97.64 | 364.1 ± 0.3 | 1.86 |
| 1160 | 0.166 | 6.357 | 1.601 | 0.530 | 99.0 | 32.792 | 99.31 | 364.4 ± 0.2 | 7.55 |
| 1400 | 0.149 | 28.53 | 0.664 | 0.225 | 98.0 | 33.190 | 100.00 | 368.4 ± 0.7 | 81.6 |
| Total | 31.55 | 111.30 | 95.85 | 32.60 | | 33.012 | | 366.6 ± 0.4 | |

$\lambda = 5.543 \times 10^{-10}\ a^{-1}$, $J = 6.8251 \times 10^{-3}$, Flux monitor GA-1550 biotite (97.9 ± 0.7 Ma in age)

$^{40}Ar$-$^{39}Ar$ age spectrum of sample A95JS130 Muscovite.

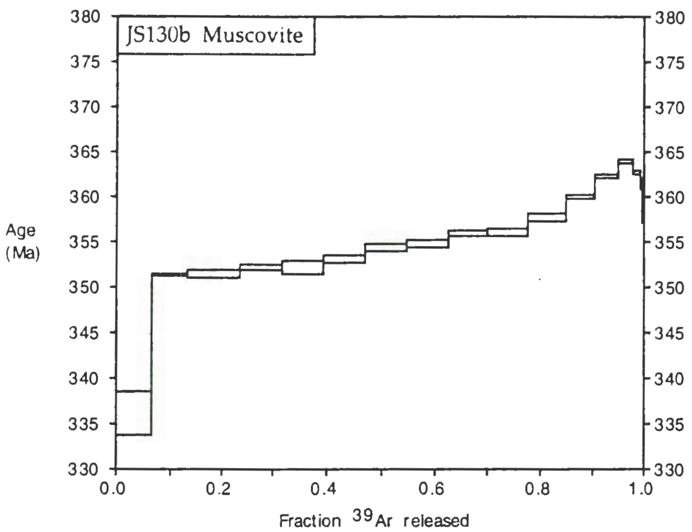


$^{40}Ar$-$^{39}Ar$ step heating data for sample A95JS130 Muscovite.

| Temp (°C) | $^{36}Ar$ (x$10^{-16}$ mol) | $^{37}Ar$ (x$10^{-16}$ mol) | $^{39}Ar$ (x$10^{-13}$ mol) | $^{40}Ar$ (x$10^{-11}$ mol) | $^{40}Ar^*$ (%) | $\frac{^{40}Ar^*}{^{39}K}$ | Cumulative $^{39}Ar$(%) | Age (Ma) ($\pm 1\sigma$) | $\frac{Ca}{K}$ (x$10^{-3}$) |
|---|---|---|---|---|---|---|---|---|---|
| 700 | 17.850 | 134.700 | 8.203 | 2.504 | 97.8 | 29.862 | 6.55 | 336.2 ± 2.4 | 31.20 |
| 750 | 3.618 | 24.690 | 8.371 | 2.637 | 99.5 | 31.352 | 13.23 | 351.4 ± 0.1 | 5.61 |
| 800 | 3.357 | 20.250 | 12.860 | 4.045 | 99.7 | 31.351 | 23.50 | 351.4 ± 0.4 | 2.99 |
| 820 | 1.132 | 8.075 | 10.210 | 3.216 | 99.8 | 31.427 | 31.65 | 352.2 ± 0.4 | 1.50 |
| 840 | 2.280 | 17.970 | 9.385 | 2.958 | 99.7 | 31.420 | 39.14 | 352.1 ± 0.7 | 3.64 |
| 860 | 1.037 | 0.653 | 9.877 | 3.119 | 99.8 | 31.523 | 47.03 | 353.2 ± 0.4 | 0.13 |
| 880 | 0.050 | 0.946 | 9.809 | 3.106 | 99.9 | 31.640 | 54.86 | 354.4 ± 0.4 | 0.18 |
| 900 | 0.994 | 0.938 | 9.710 | 3.082 | 99.8 | 31.682 | 62.61 | 354.8 ± 0.4 | 0.18 |
| 920 | 0.328 | 0.613 | 8.836 | 2.813 | 99.9 | 31.796 | 69.66 | 355.9 ± 0.2 | 0.13 |
| 950 | 1.449 | 12.540 | 10.020 | 3.194 | 99.8 | 31.804 | 77.66 | 356.0 ± 0.4 | 2.38 |
| 980 | 0.327 | 4.928 | 8.934 | 2.860 | 99.9 | 31.971 | 84.79 | 357.7 ± 0.5 | 1.05 |
| 1010 | 1.691 | 11.930 | 7.146 | 2.307 | 99.7 | 32.191 | 90.50 | 359.9 ± 0.2 | 3.17 |
| 1040 | 1.047 | 2.761 | 5.823 | 1.892 | 99.8 | 32.416 | 95.15 | 362.2 ± 0.2 | 0.90 |
| 1060 | 0.033 | 15.050 | 3.317 | 1.082 | 99.9 | 32.587 | 97.79 | 364.0 ± 0.1 | 8.62 |
| 1080 | 0.605 | 6.450 | 1.725 | 0.562 | 99.6 | 32.464 | 99.17 | 362.7 ± 0.3 | 7.11 |
| 1100 | 0.408 | 14.040 | 0.713 | 0.232 | 99.4 | 32.340 | 99.74 | 361.5 ± 0.7 | 37.40 |
| 1400 | 1.116 | 229.800 | 0.327 | 0.108 | 97.1 | 32.049 | 100.00 | 358.5 ± 1.4 | 1340.00 |
| Total | 37.32 | 506.30 | 125.30 | 39.72 | | 31.591 | | 353.9 ± 0.5 | |

$\lambda = 5.543 \times 10^{-10}\ a^{-1}$, $J = 6.8594 \times 10^{-3}$, Flux monitor GA-1550 biotite (97.9 ± 0.7 Ma in age)

$^{40}Ar$-$^{39}Ar$ age spectrum of sample A95PP192b Muscovite.

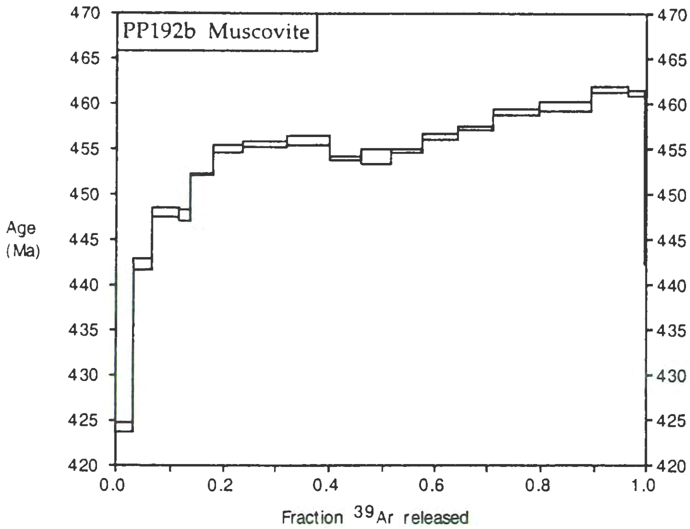


$^{40}Ar$-$^{39}Ar$ step heating data for sample A95PP192b Muscovite.

| Temp (°C) | $^{36}Ar$ (x$10^{-16}$ mol) | $^{37}Ar$ (x$10^{-16}$ mol) | $^{39}Ar$ (x$10^{-13}$ mol) | $^{40}Ar$ (x$10^{-11}$ mol) | $^{40}Ar^*$ (%) | $\frac{^{40}Ar^*}{^{39}K}$ | Cumulative $^{39}Ar$(%) | Age (Ma) (± 1σ) | $\frac{Ca}{K}$ (x$10^{-3}$) |
|---|---|---|---|---|---|---|---|---|---|
| 750 | 18.150 | 24.400 | 2.584 | 1.046 | 94.8 | 38.374 | 3.32 | 424.4 ± 0.5 | 17.90 |
| 800 | 4.634 | 8.169 | 2.536 | 1.034 | 98.6 | 40.211 | 6.57 | 442.4 ± 0.6 | 6.12 |
| 850 | 8.041 | 15.900 | 3.909 | 1.619 | 98.5 | 40.788 | 11.58 | 448.0 ± 0.5 | 7.73 |
| 870 | 4.422 | 20.020 | 1.747 | 0.725 | 98.1 | 40.757 | 13.83 | 447.7 ± 0.7 | 21.80 |
| 890 | 8.846 | 6.853 | 3.126 | 1.315 | 97.9 | 41.218 | 17.84 | 452.2 ± 0.2 | 4.17 |
| 910 | 10.630 | 5.373 | 4.547 | 1.920 | 98.3 | 41.513 | 23.67 | 455.0 ± 0.4 | 2.25 |
| 930 | 9.831 | 0.830 | 6.518 | 2.740 | 98.9 | 41.567 | 32.04 | 455.6 ± 0.4 | 0.24 |
| 950 | 4.444 | 1.253 | 6.209 | 2.598 | 99.4 | 41.602 | 40.00 | 455.9 ± 0.6 | 0.38 |
| 970 | 5.422 | 0.831 | 4.776 | 1.994 | 99.1 | 41.400 | 46.13 | 453.9 ± 0.2 | 0.33 |
| 1000 | 5.270 | 4.900 | 4.311 | 1.803 | 99.1 | 41.432 | 51.66 | 454.2 ± 0.9 | 2.16 |
| 1030 | 6.909 | 0.881 | 4.702 | 1.973 | 98.9 | 41.492 | 57.69 | 454.8 ± 0.2 | 0.36 |
| 1060 | 7.304 | 0.882 | 4.966 | 2.091 | 98.9 | 41.647 | 64.07 | 456.3 ± 0.3 | 0.34 |
| 1080 | 8.265 | 0.126 | 5.407 | 2.283 | 98.9 | 41.742 | 71.00 | 457.2 ± 0.2 | 0.04 |
| 1100 | 6.313 | 0.896 | 6.791 | 2.868 | 99.3 | 41.930 | 79.72 | 459.1 ± 0.3 | 0.25 |
| 1120 | 5.689 | 62.860 | 7.487 | 3.163 | 99.4 | 41.997 | 89.32 | 459.7 ± 0.5 | 16.00 |
| 1140 | 1.663 | 3.979 | 5.558 | 2.351 | 99.7 | 42.189 | 96.46 | 461.6 ± 0.3 | 1.36 |
| 1160 | 1.499 | 22.340 | 2.490 | 1.054 | 99.5 | 42.145 | 99.65 | 461.1 ± 0.4 | 17.10 |
| 1400 | 1.904 | 469.000 | 0.273 | 0.116 | 95.5 | 40.541 | 100.00 | 445.6 ± 3.3 | 3260.00 |
| Total | 119.20 | 649.50 | 77.94 | 32.70 | | 41.473 | | 454.6 ± 0.4 | |

$\lambda = 5.543 \times 10^{-10}\ a^{-1}$, $J = 6.9108 \times 10^{-3}$, Flux monitor GA-1550 biotite (97.9 ± 0.7 Ma in age)

# APPENDIX V

## $^{40}Ar$-$^{39}Ar$ and Rb-Sr on biotite and muscovite associated with shear zones

$^{40}Ar$-$^{39}Ar$ age spectrum of sample A95PL230b Biotite.

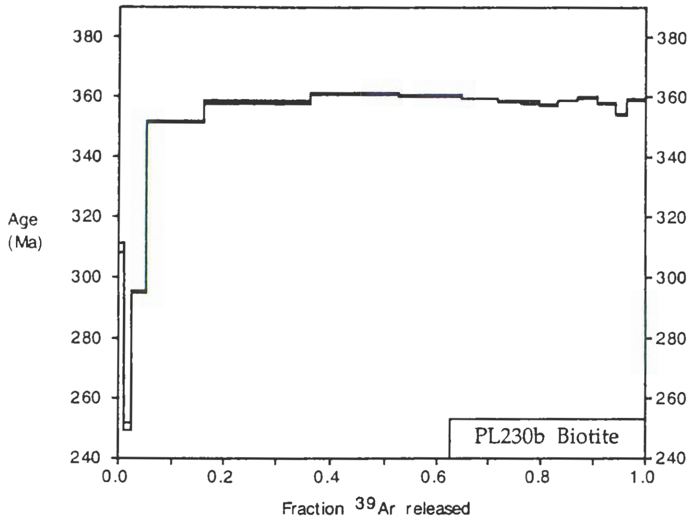


$^{40}Ar$-$^{39}Ar$ step heating data for sample A95PL230b Biotite.

| Temp (°C) | $^{36}Ar$ ($\times 10^{-16}$ mol) | $^{37}Ar$ ($\times 10^{-16}$ mol) | $^{39}Ar$ ($\times 10^{-13}$ mol) | $^{40}Ar$ ($\times 10^{-11}$ mol) | $^{40}Ar^*$ (%) | $\frac{^{40}Ar^*}{^{39}K}$ | Cumulative $^{39}Ar$(%) | Age (Ma) ($\pm 1\sigma$) | $\frac{Ca}{K}$ ($\times 10^{-3}$) |
|---|---|---|---|---|---|---|---|---|---|
| 550 | 117.400 | 8.980 | 1.227 | 0.675 | 48.6 | 26.716 | 1.16 | 309.8 ± 1.7 | 13.90 |
| 600 | 67.390 | 1.215 | 1.216 | 0.458 | 56.4 | 21.235 | 2.32 | 250.4 ± 1.3 | 1.90 |
| 650 | 191.000 | 73.360 | 3.277 | 1.396 | 59.5 | 25.363 | 5.43 | 295.3 ± 0.4 | 42.50 |
| 700 | 228.400 | 1.800 | 11.260 | 4.134 | 83.6 | 30.689 | 16.11 | 351.7 ± 0.5 | 0.30 |
| 750 | 78.840 | 3.991 | 21.070 | 6.835 | 96.5 | 31.304 | 36.10 | 358.1 ± 0.4 | 0.36 |
| 780 | 22.640 | 17.980 | 17.560 | 5.614 | 98.7 | 31.568 | 52.75 | 360.8 ± 0.4 | 1.95 |
| 810 | 14.540 | 145.400 | 12.510 | 3.989 | 98.8 | 31.516 | 64.61 | 360.3 ± 0.4 | 22.10 |
| 840 | 7.598 | 1.219 | 7.198 | 2.287 | 98.9 | 31.431 | 71.44 | 359.4 ± 0.3 | 0.32 |
| 870 | 4.447 | 31.920 | 4.979 | 1.574 | 99.1 | 31.330 | 76.16 | 358.3 ± 0.3 | 12.20 |
| 900 | 2.887 | 14.560 | 3.841 | 1.212 | 99.2 | 31.313 | 79.81 | 358.1 ± 0.3 | 7.21 |
| 930 | 3.849 | 31.780 | 3.581 | 1.131 | 98.9 | 31.232 | 83.20 | 357.3 ± 0.2 | 16.90 |
| 960 | 4.351 | 39.280 | 3.988 | 1.266 | 98.9 | 31.388 | 86.99 | 358.9 ± 0.1 | 18.70 |
| 990 | 4.103 | 37.200 | 4.142 | 1.317 | 99.0 | 31.473 | 90.92 | 359.8 ± 0.4 | 17.10 |
| 1020 | 4.982 | 1.232 | 3.542 | 1.124 | 98.6 | 31.280 | 94.28 | 357.8 ± 0.2 | 0.66 |
| 1050 | 4.354 | 51.620 | 2.400 | 0.756 | 98.2 | 30.941 | 96.55 | 354.3 ± 0.3 | 40.90 |
| 1400 | 6.000 | 667.700 | 3.636 | 1.159 | 98.4 | 31.398 | 100.00 | 359.0 ± 0.2 | 349.00 |
| Total | 762.70 | 1129.00 | 105.40 | 34.93 | | 30.965 | | 354.5 ± 0.4 | |

$\lambda = 5.543 \times 10^{-10}\ a^{-1}$, $J = 7.0132 \times 10^{-3}$, Flux monitor GA-1550 biotite (97.9 ± 0.7 Ma in age)

$^{40}Ar$-$^{39}Ar$ age spectrum of sample A95PL230b Muscovite.

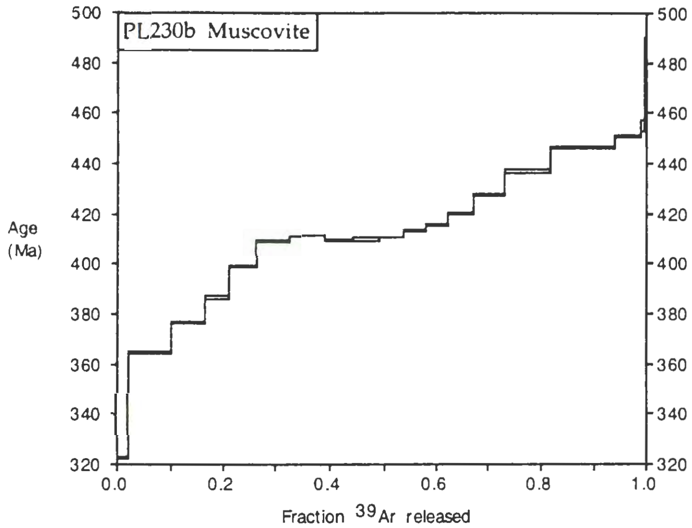


$^{40}Ar$-$^{39}Ar$ step heating data for sample A95PL230b Muscovite.

| Temp (°C) | $^{36}Ar$ ($\times10^{-16}$ mol) | $^{37}Ar$ ($\times10^{-15}$ mol) | $^{39}Ar$ ($\times10^{-13}$ mol) | $^{40}Ar$ ($\times10^{-11}$ mol) | $^{40}Ar^*$ (%) | $\frac{^{40}Ar^*}{^{39}K}$ | Cumulative $^{39}Ar$(%) | Age (Ma) ($\pm 1\sigma$) | $\frac{Ca}{K}$ ($\times10^{-2}$) |
|---|---|---|---|---|---|---|---|---|---|
| 650 | 11.100 | 13.880 | 1.196 | 0.354 | 90.7 | 26.838 | 2.03 | 322.5 ± 0.5 | 22.00 |
| 800 | 4.490 | 21.950 | 4.800 | 1.490 | 99.0 | 30.736 | 10.16 | 364.9 ± 0.2 | 8.69 |
| 850 | 4.387 | 9.618 | 3.792 | 1.221 | 98.9 | 31.824 | 16.59 | 376.5 ± 0.2 | 4.82 |
| 870 | 3.235 | 8.353 | 2.534 | 0.841 | 98.8 | 32.790 | 20.89 | 386.8 ± 0.7 | 6.26 |
| 890 | 4.705 | 7.913 | 3.174 | 1.093 | 98.7 | 33.965 | 26.27 | 399.2 ± 0.3 | 4.74 |
| 910 | 4.859 | 7.300 | 3.736 | 1.320 | 98.8 | 34.931 | 32.60 | 409.4 ± 0.3 | 3.71 |
| 930 | 2.889 | 6.136 | 3.657 | 1.294 | 99.3 | 35.126 | 38.80 | 411.4 ± 0.3 | 3.19 |
| 950 | 2.875 | 4.982 | 3.197 | 1.126 | 99.2 | 34.946 | 44.22 | 409.5 ± 0.3 | 2.96 |
| 970 | 2.140 | 5.392 | 2.905 | 1.023 | 99.3 | 34.979 | 49.14 | 409.9 ± 0.5 | 3.53 |
| 990 | 2.389 | 4.531 | 2.697 | 0.953 | 99.2 | 35.064 | 53.71 | 410.8 ± 0.2 | 3.19 |
| 1010 | 1.663 | 4.340 | 2.548 | 0.906 | 99.4 | 35.338 | 58.03 | 413.6 ± 0.5 | 3.24 |
| 1030 | 2.607 | 6.405 | 2.412 | 0.865 | 99.0 | 35.531 | 62.12 | 415.7 ± 0.3 | 5.05 |
| 1060 | 3.548 | 8.063 | 2.857 | 1.039 | 98.9 | 35.969 | 66.96 | 420.2 ± 0.3 | 5.36 |
| 1090 | 3.539 | 10.740 | 3.560 | 1.317 | 99.1 | 36.673 | 73.00 | 427.5 ± 0.2 | 5.73 |
| 1120 | 3.861 | 13.920 | 5.086 | 1.924 | 99.3 | 37.583 | 81.62 | 437.0 ± 0.6 | 5.20 |
| 1150 | 3.086 | 17.610 | 7.329 | 2.834 | 99.6 | 38.520 | 94.04 | 446.6 ± 0.3 | 4.56 |
| 1170 | 0.742 | 16.000 | 2.867 | 1.119 | 99.7 | 38.930 | 98.90 | 450.8 ± 0.5 | 10.60 |
| 1200 | 0.097 | 24.710 | 0.496 | 0.195 | 99.9 | 39.355 | 99.74 | 455.2 ± 2.3 | 94.70 |
| 1400 | 1.058 | 131.200 | 0.152 | 0.065 | 97.2 | 42.221 | 100.00 | 484.2 ± 6.2 | 1650.00 |
| Total | 63.26 | 323.10 | 59.00 | 20.98 | | 35.225 | | 412.5 ± 0.4 | |

$\lambda = 5.543 \times 10^{-10}\ a^{-1}$, $J = 7.2924 \times 10^{-3}$, Flux monitor GA-1550 biotite (97.9 ± 0.7 Ma in age)

# APPENDIX VI

## $^{40}Ar$-$^{39}Ar$ and Rb-Sr on micas associated with pegmatites synchronous with deformation

$^{40}Ar$-$^{39}Ar$ age spectrum of sample A95PS082c Muscovite.

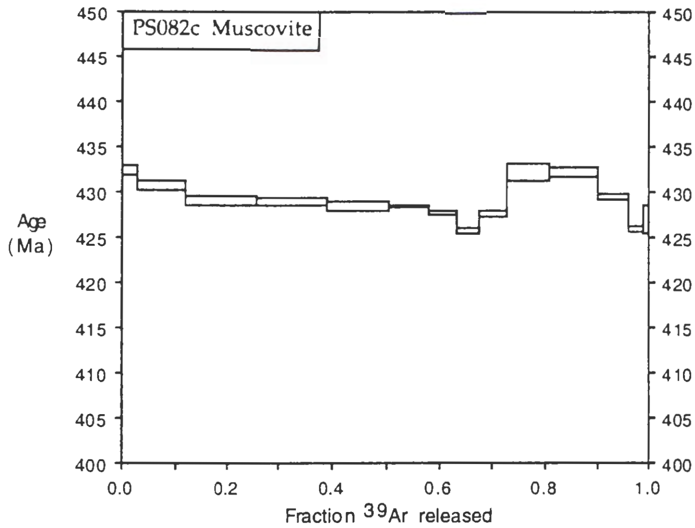


$^{40}Ar$-$^{39}Ar$ step heating data for sample A95PS082c Muscovite.

| Temp (°C) | $^{36}Ar$ ($\times10^{-15}$ mol) | $^{37}Ar$ ($\times10^{-16}$ mol) | $^{39}Ar$ ($\times10^{-13}$ mol) | $^{40}Ar$ ($\times10^{-11}$ mol) | $^{40}Ar^*$ (%) | $\frac{^{40}Ar^*}{^{39}K}$ | Cumulative $^{39}Ar$(%) | Age (Ma) ($\pm 1\sigma$) | $\frac{Ca}{K}$ ($\times10^{-4}$) |
|---|---|---|---|---|---|---|---|---|---|
| 700 | 3.001 | 0.569 | 2.269 | 0.992 | 91.0 | 39.794 | 2.95 | 432.4 ± 0.5 | 4.76 |
| 800 | 4.791 | 0.836 | 6.791 | 2.835 | 94.9 | 39.629 | 11.79 | 430.8 ± 0.5 | 2.34 |
| 850 | 6.576 | 1.168 | 10.720 | 4.426 | 95.5 | 39.449 | 25.74 | 429.0 ± 0.5 | 2.07 |
| 880 | 3.708 | 1.114 | 10.260 | 4.159 | 97.3 | 39.447 | 39.09 | 429.0 ± 0.4 | 2.06 |
| 910 | 2.529 | 0.972 | 8.751 | 3.523 | 97.8 | 39.380 | 50.48 | 428.4 ± 0.5 | 2.11 |
| 940 | 2.098 | 0.570 | 5.754 | 2.330 | 97.3 | 39.388 | 57.96 | 428.4 ± 0.2 | 1.88 |
| 970 | 2.140 | 0.571 | 3.864 | 1.583 | 95.9 | 39.314 | 62.99 | 427.7 ± 0.2 | 2.81 |
| 1000 | 2.446 | 0.572 | 3.439 | 1.418 | 94.8 | 39.107 | 67.47 | 425.7 ± 0.3 | 3.16 |
| 1030 | 2.826 | 0.572 | 4.070 | 1.684 | 95.0 | 39.306 | 72.76 | 427.6 ± 0.3 | 2.67 |
| 1060 | 4.103 | 0.573 | 5.969 | 2.497 | 95.1 | 39.779 | 80.53 | 432.2 ± 0.9 | 1.82 |
| 1080 | 3.374 | 0.847 | 7.519 | 3.093 | 96.7 | 39.785 | 90.32 | 432.3 ± 0.5 | 2.14 |
| 1100 | 1.093 | 10.640 | 4.539 | 1.826 | 98.2 | 39.498 | 96.22 | 429.5 ± 0.3 | 44.50 |
| 1120 | 0.328 | 0.580 | 1.980 | 0.785 | 98.7 | 39.132 | 98.80 | 426.0 ± 0.3 | 5.57 |
| 1400 | 0.360 | 113.300 | 0.923 | 0.373 | 97.1 | 39.236 | 100.00 | 427.0 ± 1.6 | 2330.00 |
| Total | 39.37 | 132.90 | 76.84 | 31.52 | | 39.483 | | 429.4 ± 0.5 | |

$\lambda = 5.543 \times 10^{-10}\ a^{-1}$, $J = 6.8054 \times 10^{-3}$, Flux monitor GA-1550 biotite (97.9 ± 0.7 Ma in age)

PRISE

For Attention: Alfredo Camacho
AGSO
GPO Box 378
Canberra
A.C.T. 2601

13 December 1996

Dear Alfredo

**Re: Purchase Order Number s0633**

I have completed the Rb-Sr isotopic analyses on the two muscovite samples as requested. The results are presented below.

Table 1: Summary of Rb-Sr results.

| Sample # | Rb (ppm) | $^{87}$Rb (nm/g) | Sr (ppm) | $^{86}$Sr (nm/g) | $^{87}$Rb/$^{86}$Sr | $^{87}$Sr/$^{86}$Sr * |
|---|---|---|---|---|---|---|
| PS082C | 256.8 | 836.8 | 53.24 | 59.36 | 14.0960 | 0.80529 ± 2 |
| A95AC022b | 359.9 | 1172.6 | 29.36 | 32.30 | 36.3083 | 0.94726 ± 2 |

Notes: (1) * Measured, present-day $^{87}$Sr/$^{86}$Sr ratios (± 2σ), normalised to $^{86}$Sr/$^{88}$Sr = 0.1194;
(2) The $^{87}$Sr/$^{86}$Sr value for the NBS Sr isotope standard (SRM 987 ) run with these samples was 0.710191 ± 23 (± 2σ).

Yours sincerely

Dr RICHARD ARMSTRONG

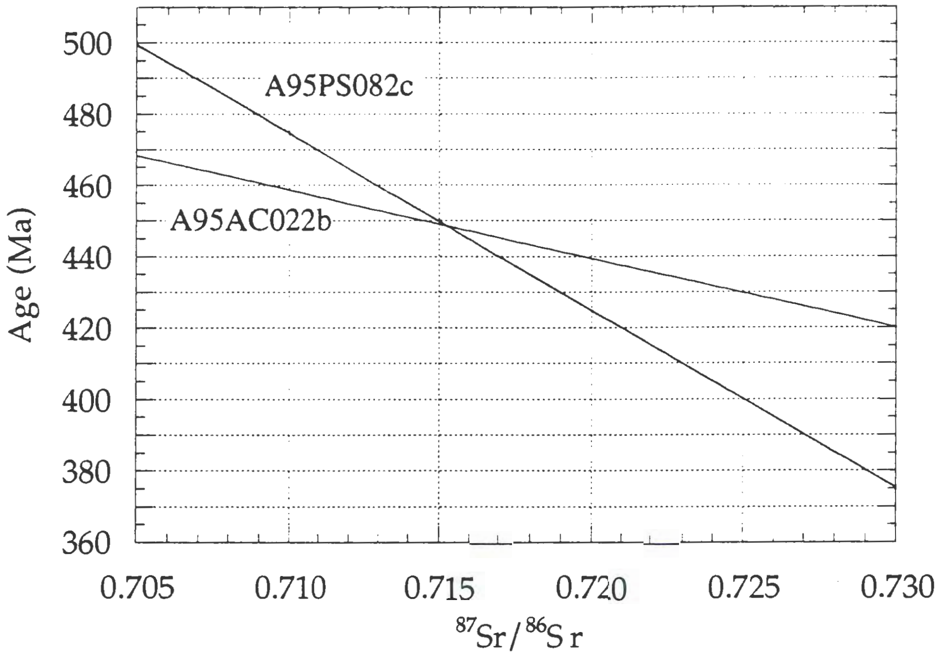


Growth curves for samples PS082c and AC022b showing the Rb-Sr age decreasing with increasing $^{87}Sr/^{86}Sr$